

State of the Art of Batteries of the 4th Generation

N. Wagner, N.A. Cañas, D. Wittmaier and K.A. Friedrich

**German Aerospace Center, Institute for Engineering
Thermodynamics, Pfaffenwaldring 38-40, 70569 Stuttgart, Germany**

**8th International Workshop on Impedance Spectroscopy (IWIS)
23-25 September, Chemnitz, Germany**

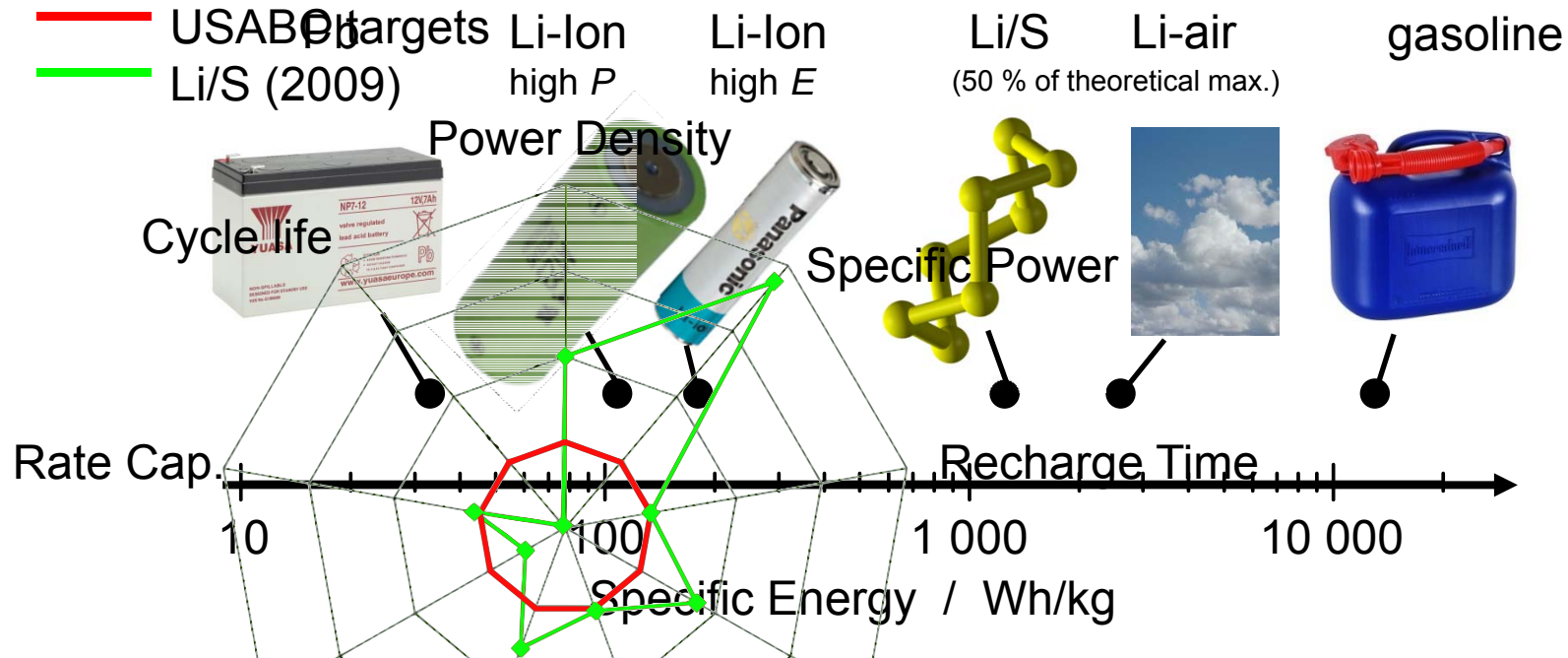


Presentation outline

- Introduction and motivation
 - Definition 4th generation batteries
 - Examples of batteries and applications
- Metal-Sulfur Batteries
 - Li-Sulfur and Mg-Sulfur Batteries
 - Production technique
 - Characterization
- Metal-Air Batteries
 - Li-Air and Zn-Air Batteries
 - Production techniques at the DLR
 - Characterization
- Outlook



Novel Battery Concepts – Specific Energy Potentials



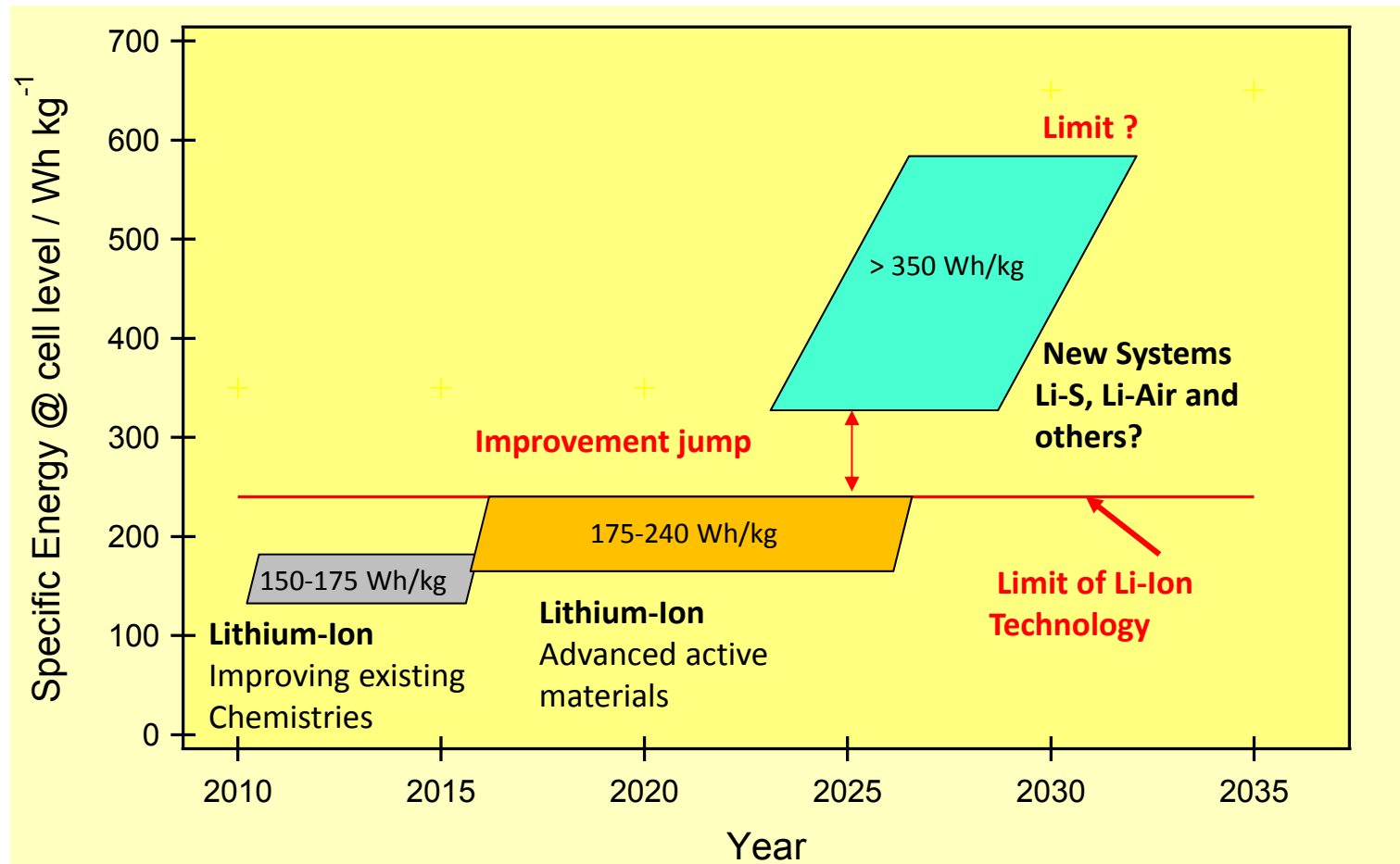
Upper T

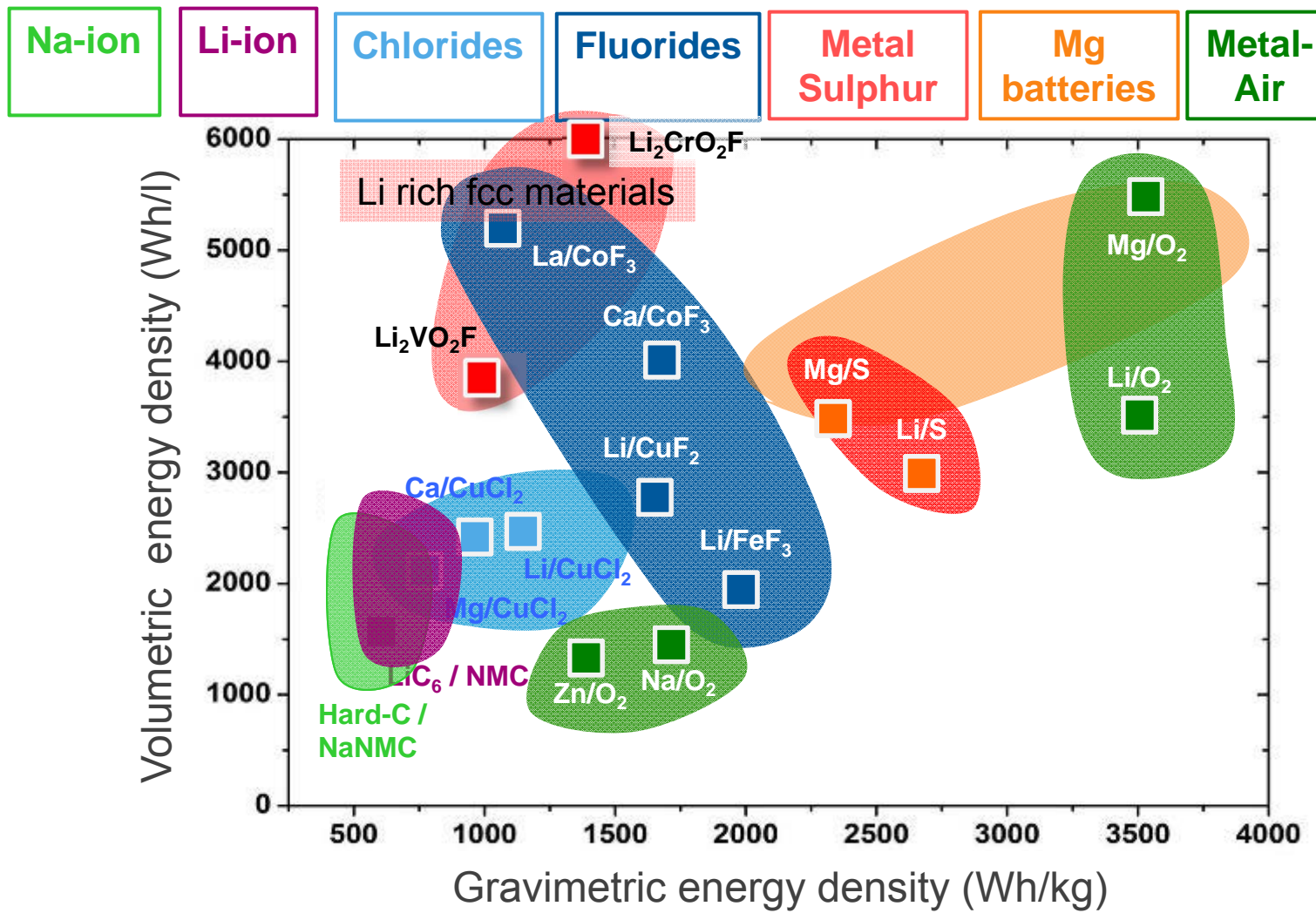
Chemistry	Cell size	Wh/L *theory	Wh/L actual	% achieved	Wh/kg *theory	Wh/kg actual	% achieved
LiFePO ₄	54208	1980	292	14.8	587	156	26.6
LiFePO ₄	16650	1980	223	11.3	587	113	19.3
LiMn ₂ O ₄	26700	2060	296	14.4	500	109	21.8
LiCoO ₂	18650	2950	570	19.3	1000	250	25
Si-LiMO ₂	18650	2950	919	31.2	1000	252	25.2
Panasonic							

ation, 2009.

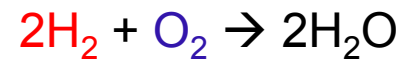


Technical Progress: Improvement of Energy Density





Chemistry of Fuel Cells and Batteries



Light →
← Heavy

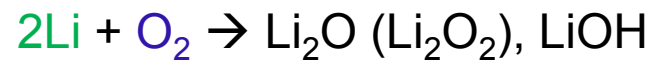
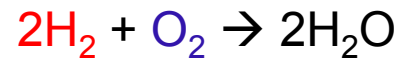
1 H 1.008	2																18 He 4.0026
3 Li 6.94	4 Be 9.0122											5 B 10.81	6 C 12.011	7 N 14.007	8 O 15.999	9 F 18.998	10 Ne 20.180
11 Na 22.990	12 Mg 24.305											13 Al 26.982	14 Si 28.085	15 P 30.974	16 S 32.06	17 Cl 35.45	18 Ar 39.948
19 K 39.098	20 Ca 40.078	21 Sc 44.956	22 Ti 47.867	23 V 50.942	24 Cr 51.996	25 Mn 54.938	26 Fe 55.845	27 Co 58.933	28 Ni 58.693	29 Cu 63.546	30 Zn 65.38	31 Ga 69.723	32 Ge 72.63	33 As 74.922	34 Se 78.96	35 Br 79.904	36 Kr 83.798
37 Rb 85.468	38 Sr 87.62	39 Y 88.906	40 Zr 91.224	41 Nb 92.906	42 Mo 95.96	43 Tc (98)	44 Ru 101.07	45 Rh 102.91	46 Pd 106.42	47 Ag 107.87	48 Cd 112.41	49 In 114.82	50 Sn 118.71	51 Sb 121.76	52 Te 127.60	53 I 126.90	54 Xe 131.29
55 Cs 132.91	56 Ba 137.33	57-71 *	72 Hf 178.49	73 Ta 180.95	74 W 183.84	75 Re 186.21	76 Os 190.23	77 Ir 192.22	78 Pt 195.08	79 Au 196.97	80 Hg 200.59	81 Tl 204.38	82 Pb 207.2	83 Bi 208.98	84 Po (209)	85 At (210)	86 Rn (222)
87 Fr (223)	88 Ra (226)	89-103 #	104 Rf (265)	105 Db (268)	106 Sg (271)	107 Bh (270)	108 Hs (277)	109 Mt (276)	110 Ds (281)	111 Rg (280)	112 Cn (285)	113 Uut (284)	114 Fl (289)	115 Uup (288)	116 Lv (293)	117 Uus (294)	118 Uuo (294)

Electropositive

Electronegative



Chemistry of Fuel Cells and Batteries



Light →
← Heavy

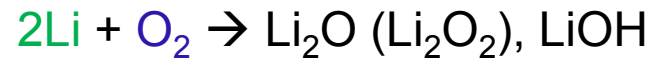
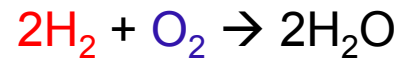
1 H 1.008	2											13 B 10.81	14 C 12.011	15 N 14.007	16 O 15.999	17 F 18.998	18 He 4.0026
3 Li 6.94	4 Be 9.0122											13 Al 26.982	14 Si 28.085	15 P 30.974	16 S 32.06	17 Cl 35.45	18 Ar 39.948
11 Na 22.990	12 Mg 24.305	3	4	5	6	7	8	9	10	11	12	13 Ga 69.723	14 Ge 72.63	15 As 74.922	16 Se 78.96	17 Br 79.904	18 Kr 83.798
19 K 39.098	20 Ca 40.078	21 Sc 44.956	22 Ti 47.867	23 V 50.942	24 Cr 51.996	25 Mn 54.938	26 Fe 55.845	27 Co 58.933	28 Ni 58.693	29 Cu 63.546	30 Zn 65.38	31 Ga 69.723	32 Ge 72.63	33 As 74.922	34 Se 78.96	35 Br 79.904	36 Kr 83.798
37 Rb 85.468	38 Sr 87.62	39 Y 88.906	40 Zr 91.224	41 Nb 92.906	42 Mo 95.96	43 Tc (98)	44 Ru 101.07	45 Rh 102.91	46 Pd 106.42	47 Ag 107.87	48 Cd 112.41	49 In 114.82	50 Sn 118.71	51 Sb 121.76	52 Te 127.60	53 I 126.90	54 Xe 131.29
55 Cs 132.91	56 Ba 137.33	57-71 *	72 Hf 178.49	73 Ta 180.95	74 W 183.84	75 Re 186.21	76 Os 190.23	77 Ir 192.22	78 Pt 195.08	79 Au 196.97	80 Hg 200.59	81 Tl 204.38	82 Pb 207.2	83 Bi 208.98	84 Po (209)	85 At (210)	86 Rn (222)
87 Fr (223)	88 Ra (226)	89-103 #	104 Rf (265)	105 Db (268)	106 Sg (271)	107 Bh (270)	108 Hs (277)	109 Mt (276)	110 Ds (281)	111 Rg (280)	112 Cn (285)	113 Uut (284)	114 Fl (289)	115 Uup (288)	116 Lv (293)	117 Uus (294)	118 Uuo (294)

Electropositive

Electronegative



Chemistry of Fuel Cells and Batteries



Light →
← Heavy

1 H 1.008	2											13 B 10.81	14 C 12.011	15 N 14.007	16 O 15.999	17 F 18.998	18 He 4.0026
3 Li 6.94	4 Be 9.0122											13 Al 26.982	14 Si 28.085	15 P 30.974	16 S 32.06	17 Cl 35.45	18 Ar 39.948
11 Na 22.990	12 Mg 24.305	3	4	5	6	7	8	9	10	11	12	13 Ga 69.723	14 Ge 72.63	15 As 74.922	16 Se 78.96	17 Br 79.904	18 Kr 83.798
19 K 39.098	20 Ca 40.078	21 Sc 44.956	22 Ti 47.867	23 V 50.942	24 Cr 51.996	25 Mn 54.938	26 Fe 55.845	27 Co 58.933	28 Ni 58.693	29 Cu 63.546	30 Zn 65.38	31 Ga 69.723	32 Ge 72.63	33 As 74.922	34 Se 78.96	35 Br 79.904	36 Kr 83.798
37 Rb 85.468	38 Sr 87.62	39 Y 88.906	40 Zr 91.224	41 Nb 92.906	42 Mo 95.96	43 Tc (98)	44 Ru 101.07	45 Rh 102.91	46 Pd 106.42	47 Ag 107.87	48 Cd 112.41	49 In 114.82	50 Sn 118.71	51 Sb 121.76	52 Te 127.60	53 I 126.90	54 Xe 131.29
55 Cs 132.91	56 Ba 137.33	57-71 *	72 Hf 178.49	73 Ta 180.95	74 W 183.84	75 Re 186.21	76 Os 190.23	77 Ir 192.22	78 Pt 195.08	79 Au 196.97	80 Hg 200.59	81 Tl 204.38	82 Pb 207.2	83 Bi 208.98	84 Po (209)	85 At (210)	86 Rn (222)
87 Fr (223)	88 Ra (226)	89-103 #	104 Rf (265)	105 Db (268)	106 Sg (271)	107 Bh (270)	108 Hs (277)	109 Mt (276)	110 Ds (281)	111 Rg (280)	112 Cn (285)	113 Uut (284)	114 Fl (289)	115 Uup (288)	116 Lv (293)	117 Uus (294)	118 Uuo (294)

Electropositive

Electronegative



Activities of the „Batterietechnik“ team at DLR

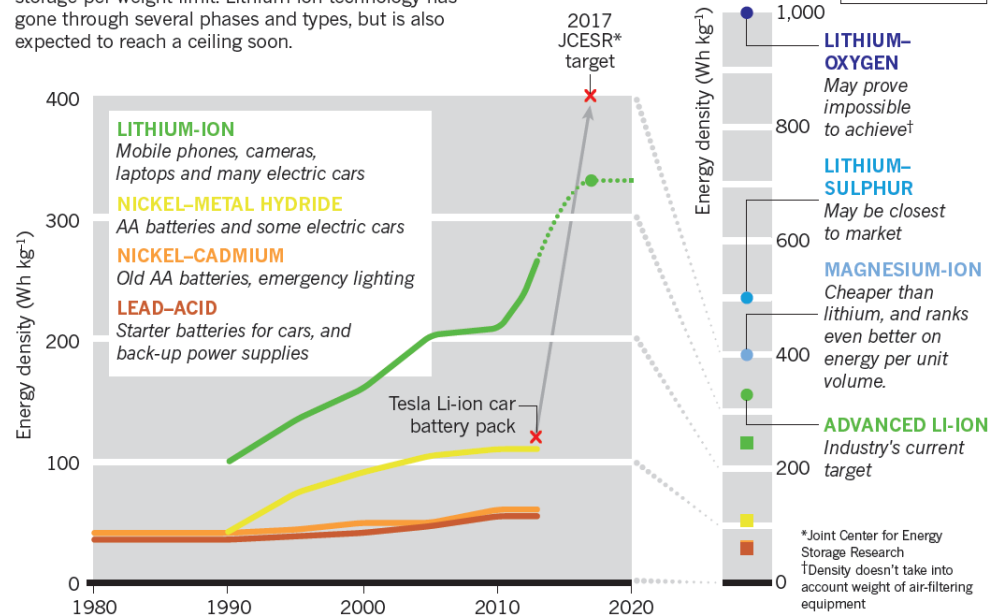
Production and Characterisation
of cathodes for

Lithium-Sulfur and
Lithium-air batteries

Characterisation of
Li-ion batteries with
in-situ and ex-situ-methods

POWERING UP

Portable rechargeable batteries tend to hit an energy-storage-per-weight limit. Lithium-ion technology has gone through several phases and types, but is also expected to reach a ceiling soon.



Source: N A T U R E | V O L 5 0 7 | 6 M A R C H 2 0 1 4



Metal-Sulfur Batteries



Metal-Sulfur Batteries: Overview

Electrochemical Reaction	ΔG	Voltage	Capacity (Cathode)	Energy density	
	kJ/mol	V	mAh/g	Wh/kg	Wh/L
$\text{Mg} + \text{S} \leftrightarrow \text{MgS}$	-341.8	1.771	1672	1684	3221
$2\text{Li} + \text{S} \leftrightarrow \text{Li}_2\text{S}$	-439.0	2.275	1672	2654	2856
$2\text{Na} + 3\text{S} \leftrightarrow \text{Na}_2\text{S}_3$	-405.2	2.100	558.4	791.7	1179
$2\text{Al} + 3\text{S} \leftrightarrow \text{Al}_2\text{S}_3$	-213.3	1.106	1672	1184	2676
$\text{Zn} + \text{S} \leftrightarrow \text{ZnS}$	-201.3	1.043	1672	573.6	2162
$\text{CoO}_2 + \text{LiC}_6 \leftrightarrow \text{LiCoO}_2 + \text{C}_6$	-347.4	3.600	273.8	567.8	1901

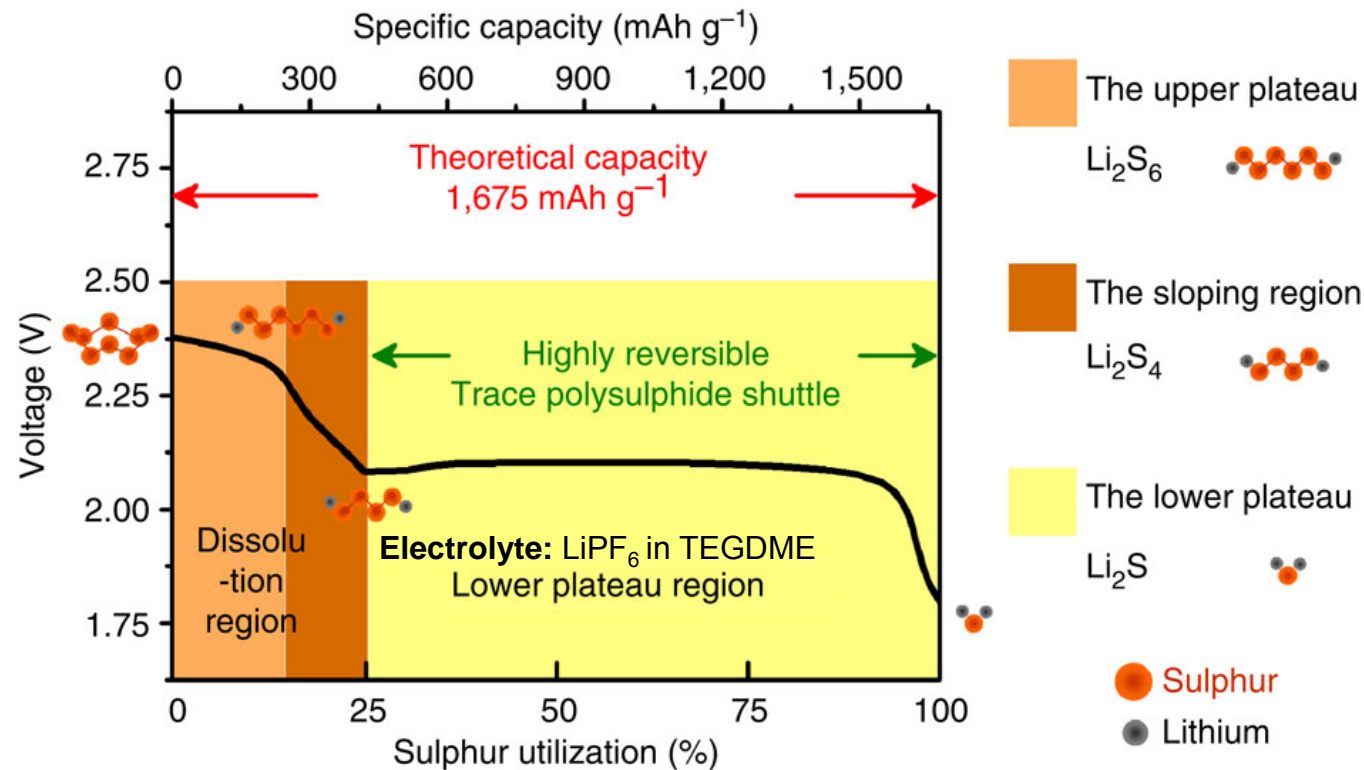


Metal-Sulfur Batterie- Summary

Electrochemical Reaction	ΔG	Voltage	Capacity (Cathode)	Energy density	
	kJ/mol	V	mAh/g	Wh/kg	Wh/L
$\text{Mg} + \text{S} \leftrightarrow \text{MgS}$	-341.8	1.771	1672	1684	3221
$2\text{Li} + \text{S} \leftrightarrow \text{Li}_2\text{S}$	-439.0	2.275	1672	2654	2856
$2\text{Na} + 3\text{S} \leftrightarrow \text{Na}_2\text{S}_3$	-405.2	2.100	558.4	791.7	1179
$2\text{Al} + 3\text{S} \leftrightarrow \text{Al}_2\text{S}_3$	-213.3	1.106	1672	1184	2676
$\text{Zn} + \text{S} \leftrightarrow \text{ZnS}$	-201.3	1.043	1672	573.6	2162
$\text{CoO}_2 + \text{LiC}_6 \leftrightarrow \text{LiCoO}_2 + \text{C}_6$	-347.4	3.600	273.8	567.8	1901



Lithium-Sulfur Battery: Electrochemistry



Y.-S. Su *et al.*, Nature (2013)

Polysulfides (Li_2S_x) are intermediates in the transition of S_8 to S^{2-}

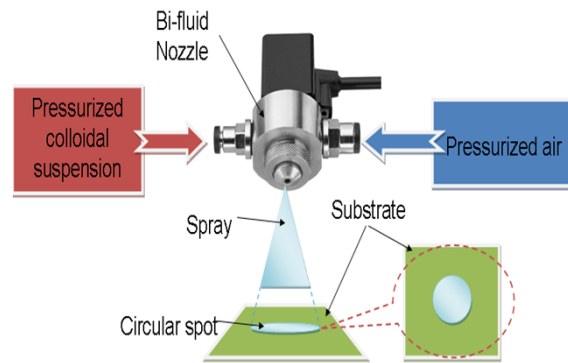


- gradual dissolution of sulfur from the cathode
- Self-discharge
- Different voltage plateaus



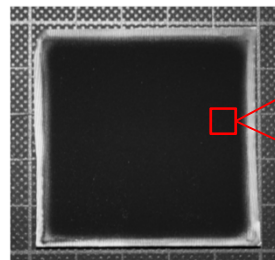
Cathode production technique at DLR-TT

Suspension-spray machine

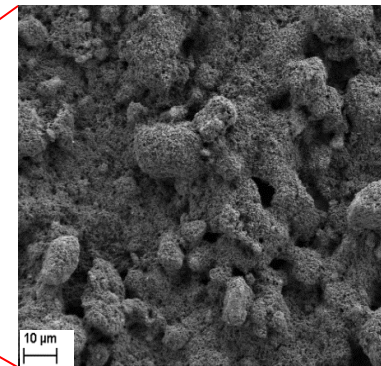


- Nozzle with extern mixing of air and suspension
- Cathode mixture: Sulfur or Sulfur/Carbon composite, Carbon Black and PVDF (50:40:10, wt.%).
Solvents: Ethanol and DMSO

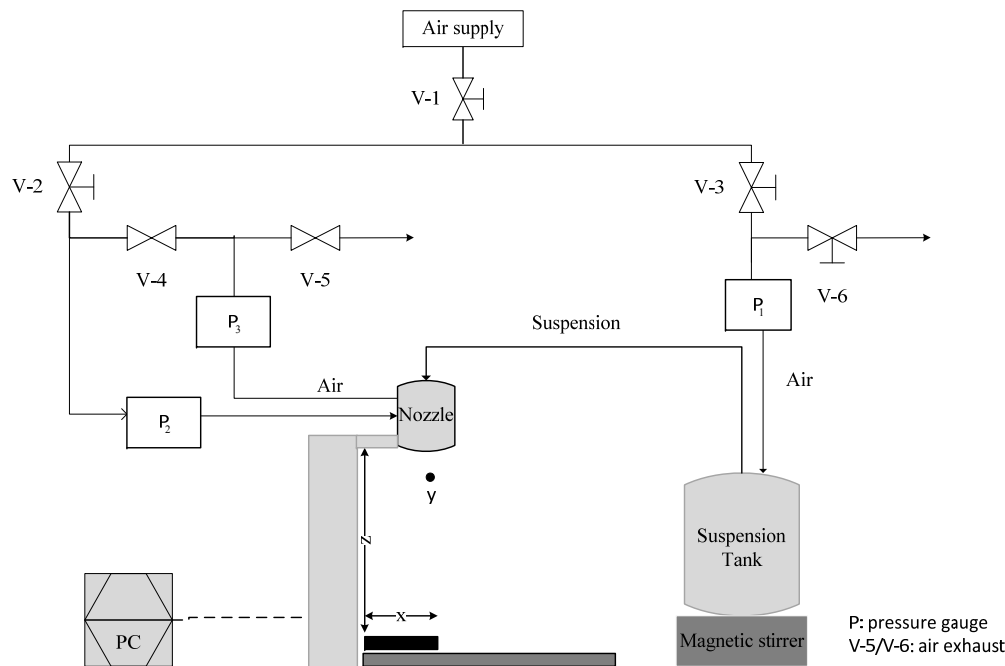
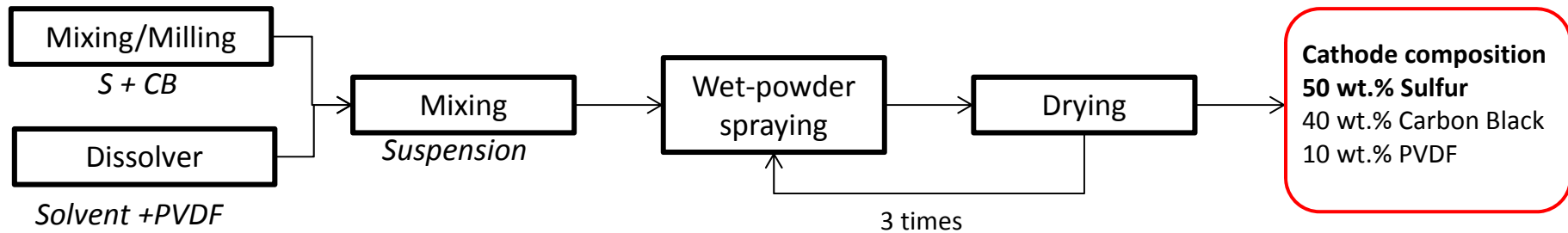
**Sprayed
cathode**



5 x 5 cm²



Wet powder spraying for electrode fabrication



Air-atomizing external mixing nozzle controlled by a 3D axis robot

The axis with the nozzle moves in perpendicular direction (y) to the substrate holder



Influence of cathode fabrication

Mixing/Milling	Coating	Drying
Initial procedure (Cathode I)		
Roll mixer [‡]	Suspension spray	In vacuum oven
1) Mix of S, CB and PVDF (5 rpm, t= 12 h)	– Internal mixing nozzle	80 °C (48 h)
2) Mix with solvents [†] (5 rpm, t= 12 h)	– Coating in one step – Heating plate under substrate (100 °C)	
New procedure (Cathode II)		
Tumbling mixer [‡]	Suspension spray	In vacuum oven
1) Mix of S and CB (20 rpm, t= 24 h)	– External mixing nozzle	Between sprayed layers,
2) Dissolution of PVDF in solvents [†] (magnet stirring)	– Coating in 3 steps or more	60 °C (1.5-3 h)
3) Mix of S and CB with dissolution (2)	– No heating plate	
(20 rpm, t = 24 h)	– Drying between each sprayed layer	At the end of coating: 60 °C (24 h) In vacuum in the glove box

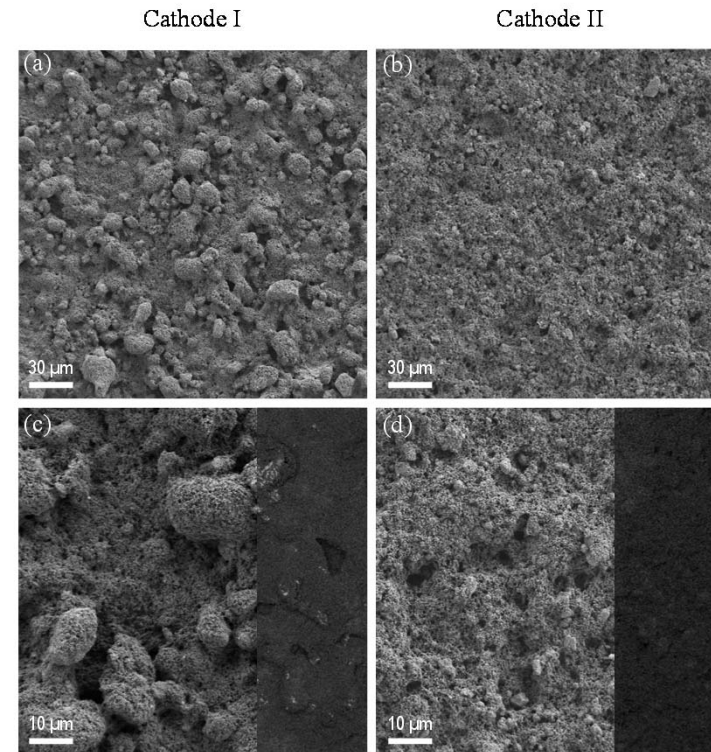
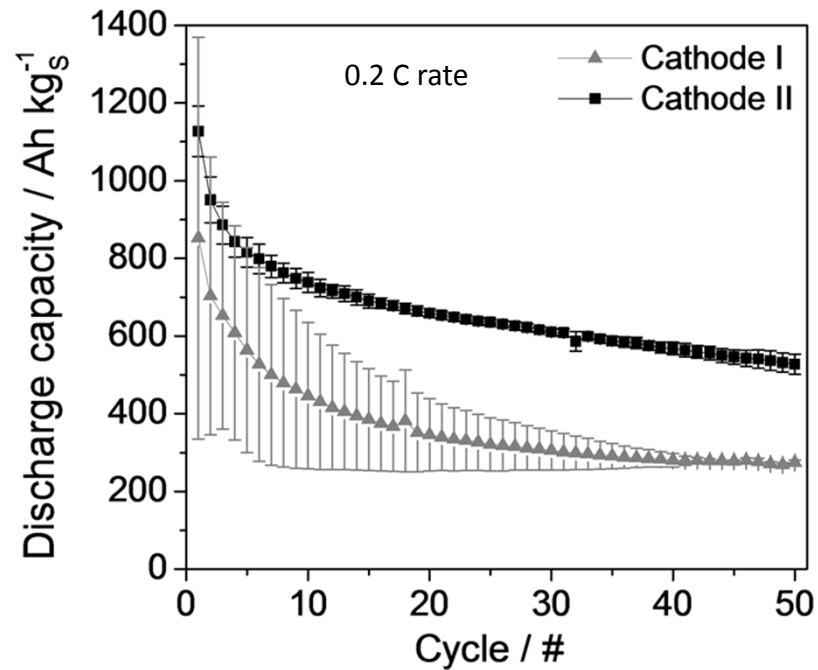
[†]Solvents: Ethanol/DMSO (50:50 wt.%). [‡]In both cases ceramic balls were added in the mixing tank.

N.A. Cañas, A.L.P. Baltazar, M.A.P. Morais, T.O. Freitag, N. Wagner, K.A. Friedrich, *Electrochim. Acta*, **157** (2015) 351-358



Influence of cathode fabrication

Cathode I ►►► Cathode II



Optimization of suspension spraying and mixing processes

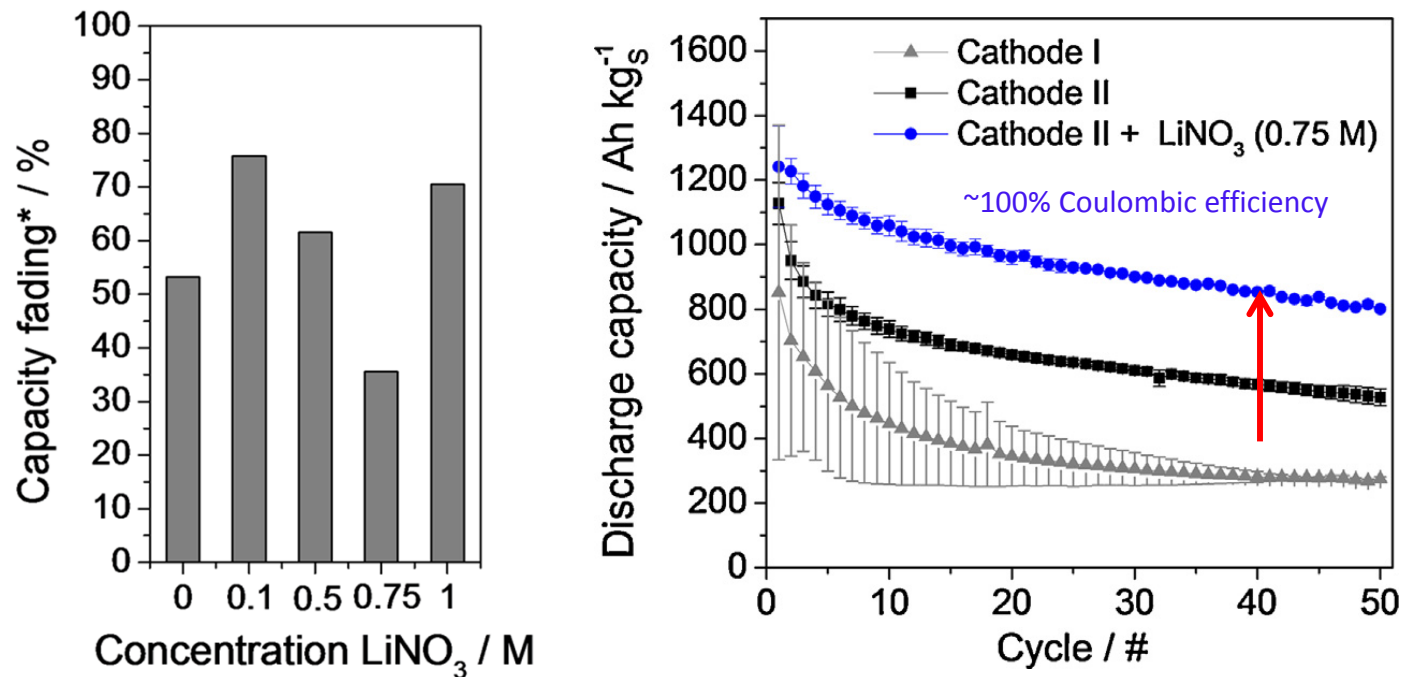
- Improved dispersion of S particles
- Reduction of S particle size

Electrolyte: 1M LiPF₆ in TEGDME



Influence of LiNO_3 as co-salt

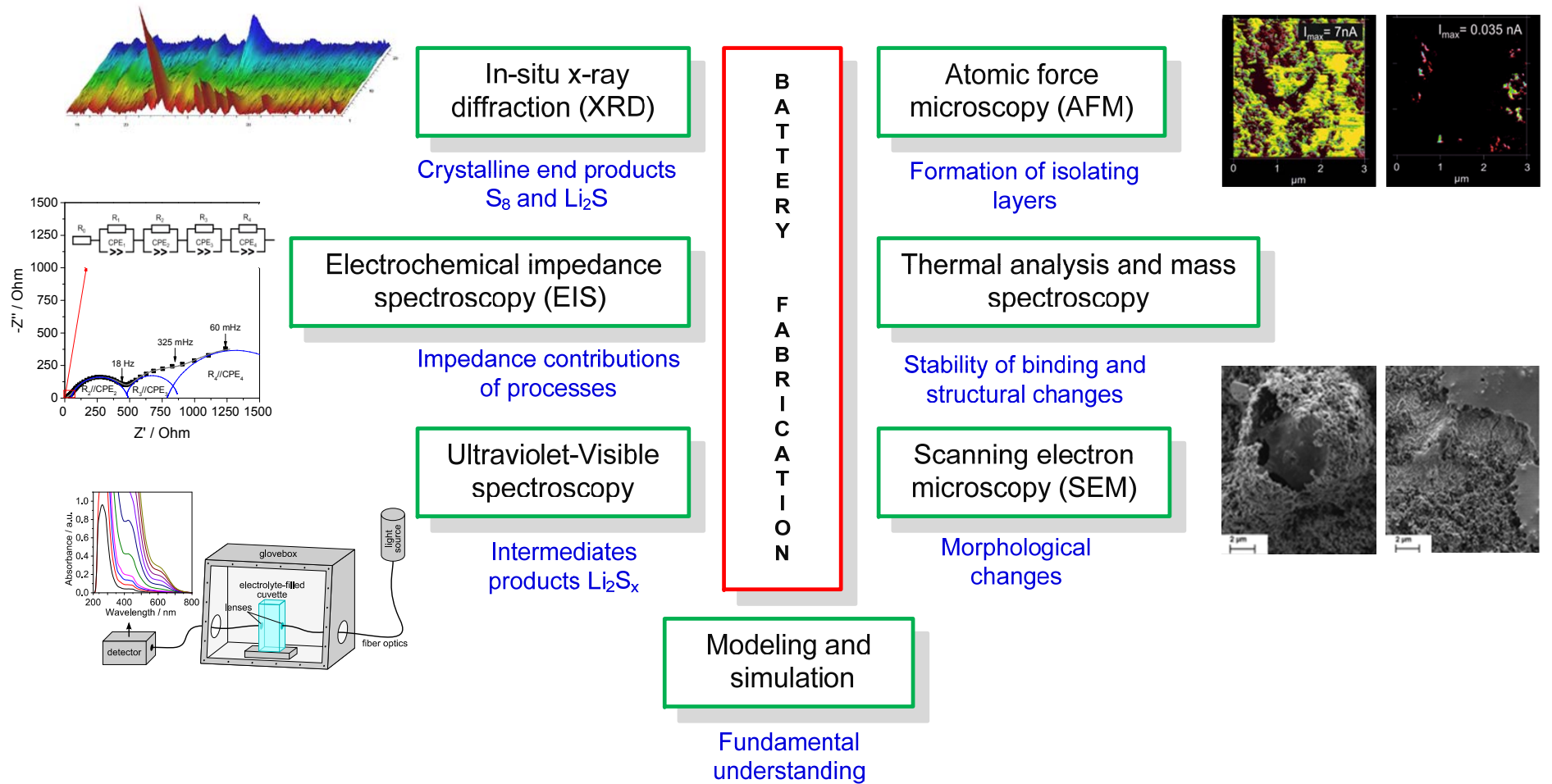
Capacity fading and coulombic efficiency is affected by the concentration of the co-salt



Considering both the capacity fading and the Coloumbic efficiency:
the optimal concentration of LiNO_3 was found to be 0.75M for this cell configuration/components

Electrolyte= 1M LiPF_6 in TEGDME

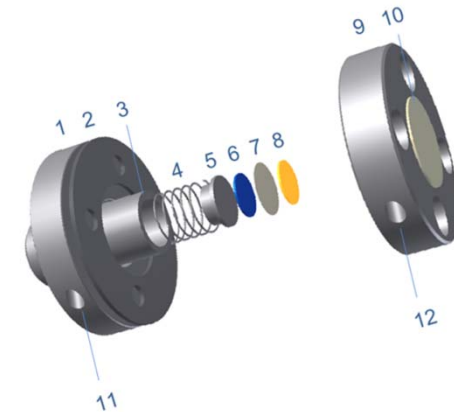
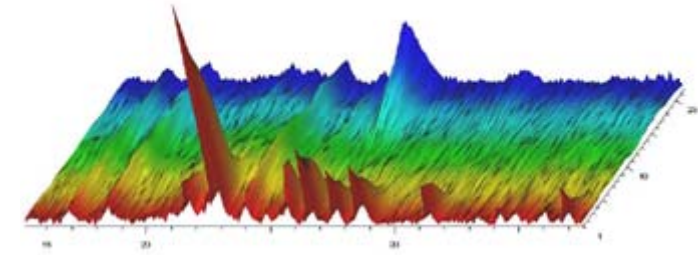
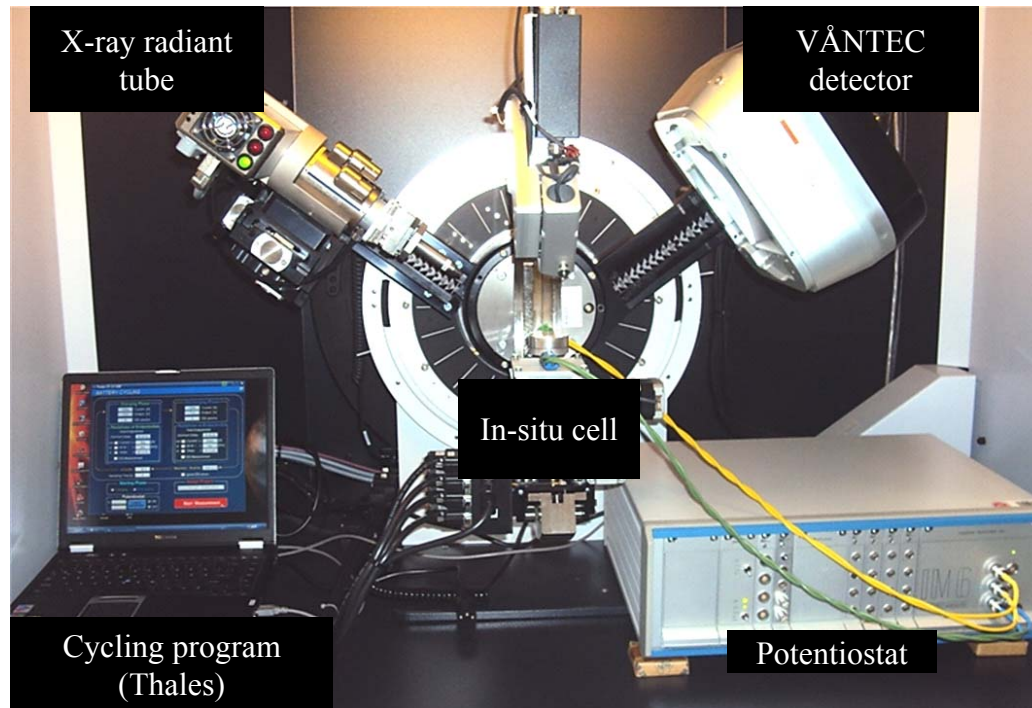
Main *in situ* and *ex situ* characterization techniques



In situ X-Ray diffraction

Objective:

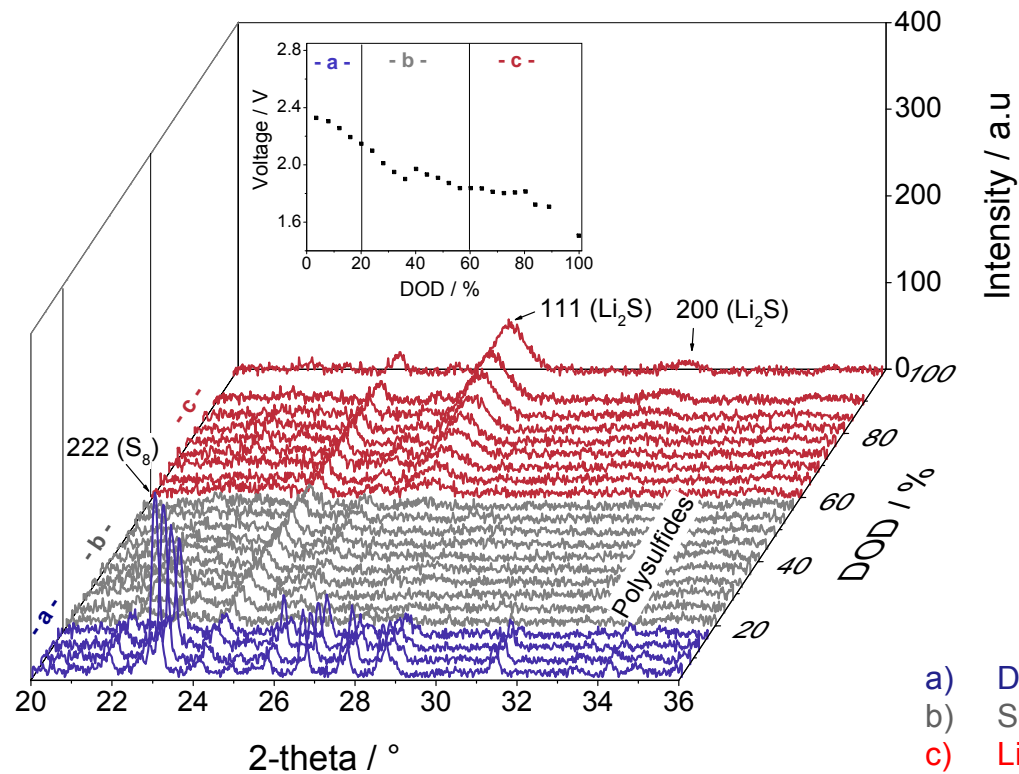
- Monitoring of crystalline reaction products of the cathode
- identification of structural changes during cycling



- 1) anode plate
- 2) polymer gasket
- 3) insulator plastic tube
- 4) spring
- 5) stainless steel anode collector
- 6) anode
- 7) separator
- 8) cathode
- 9) cathode plate
- 10) Al-window
- 11) holes for connecting the banana jacks

In situ X-Ray diffraction

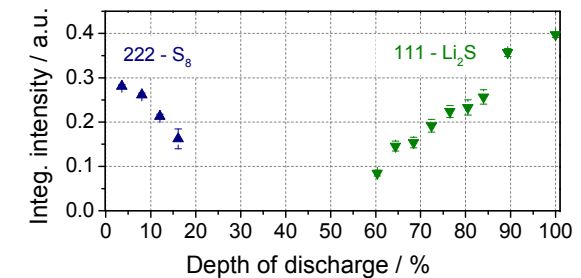
Spectra collected during discharge



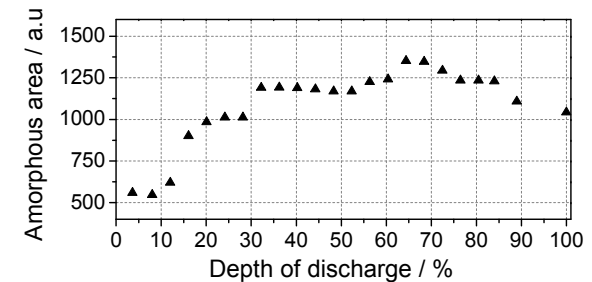
Quantification of crystalline and amorphous phase

1st discharge

(a)



(b)



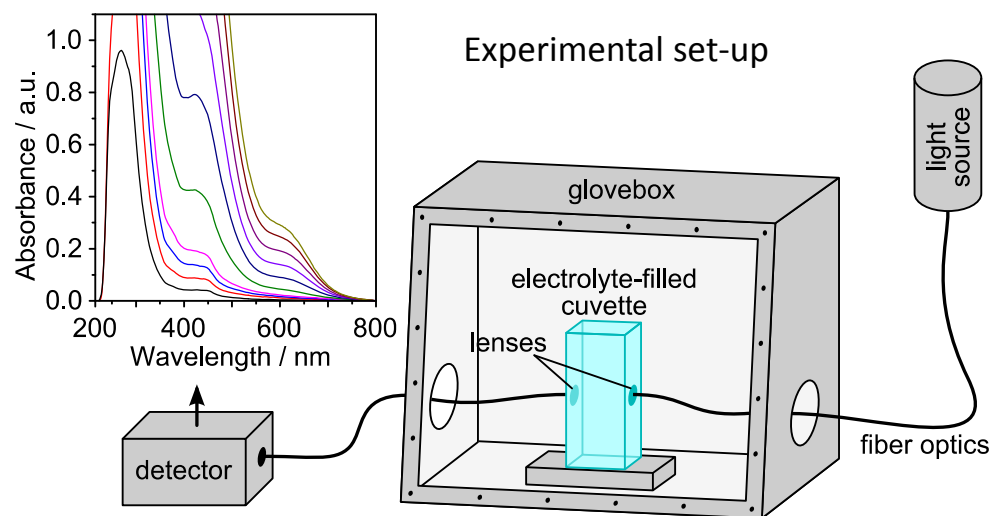
- a) Dissolution of sulfur and reduction to soluble polysulfides
- b) Soluble polysulfides
- c) Li_2S formation

N. A. Cañas, S. Wolf, N. Wagner, K. A. Friedrich. J. of Power Sources, 226 (2013) 313-319.



UV-vis spectroscopy

Investigation and quantification of reaction intermediates (polysulfides)



Wavelength /nm	Species (in TEGDME)
245, <u>255</u>, 282	$\text{S}^- (\text{Li}_2\text{S})$
243, <u>265</u>, 289	cyclo S_8
332	S_6^{2-}
425	S_4^{2-}
615	$\text{S}_3^{\cdot-}$

References:

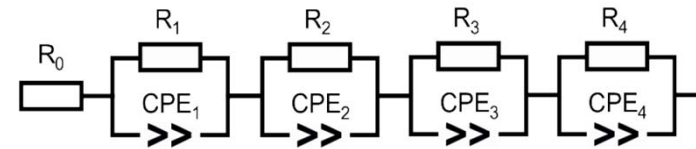
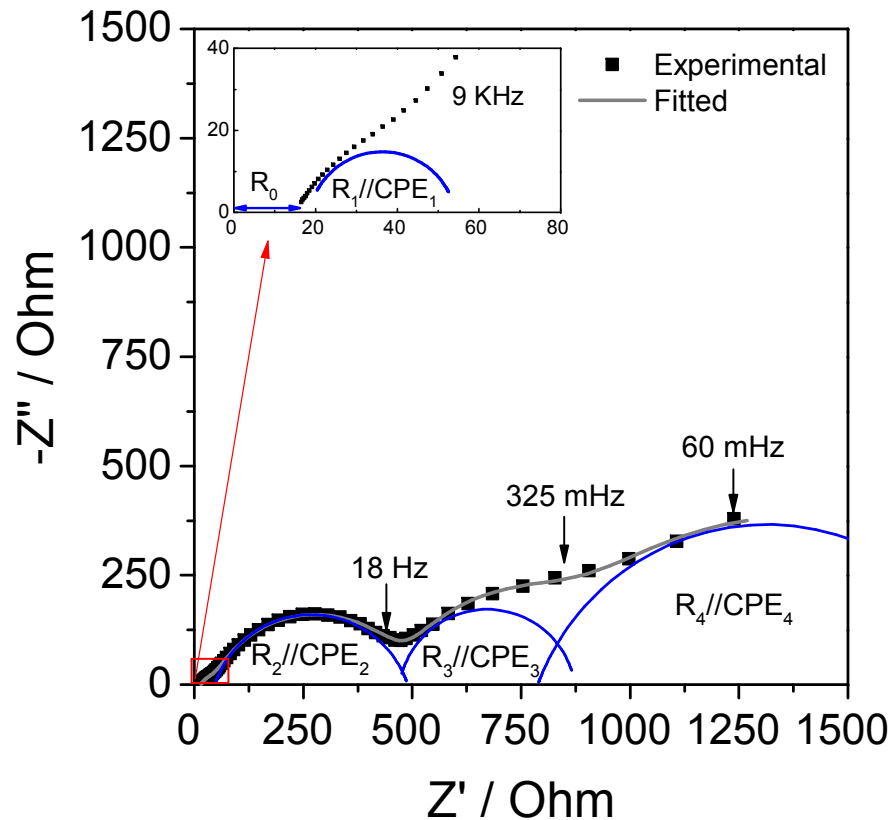
- Stoichiometric mixture of Li_2S and S_8 in TEGDME*
- Li_2S in TEGDME
- S_8 in TEGDME

*TEGDME: Tetraethylene glycol dimethyl ether



Electrochemical Impedance spectroscopy (EIS)

Investigation of physical and chemical processes during cycling

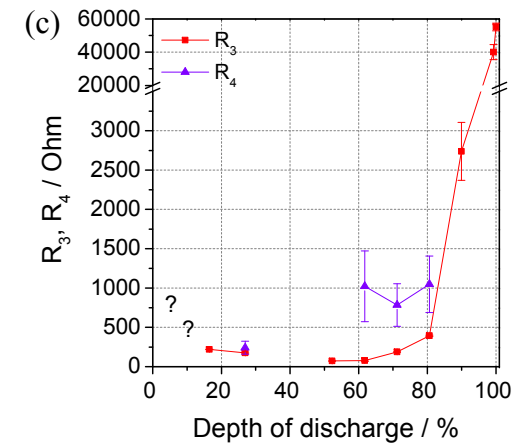
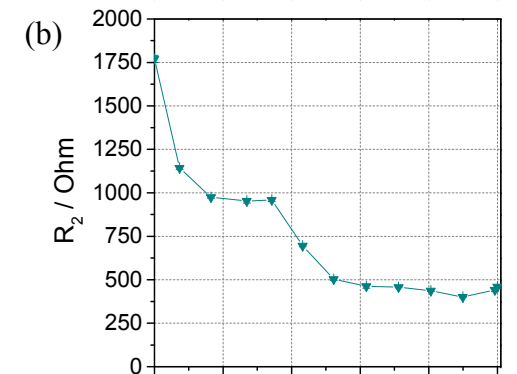
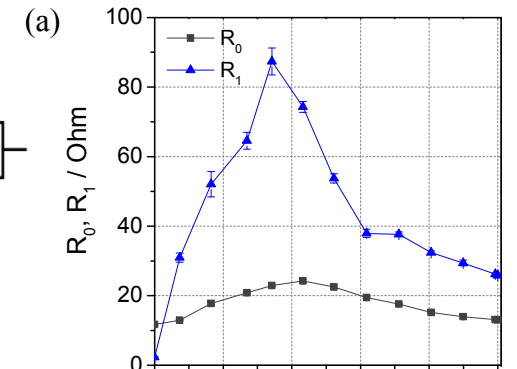
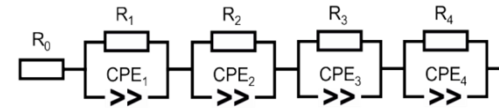
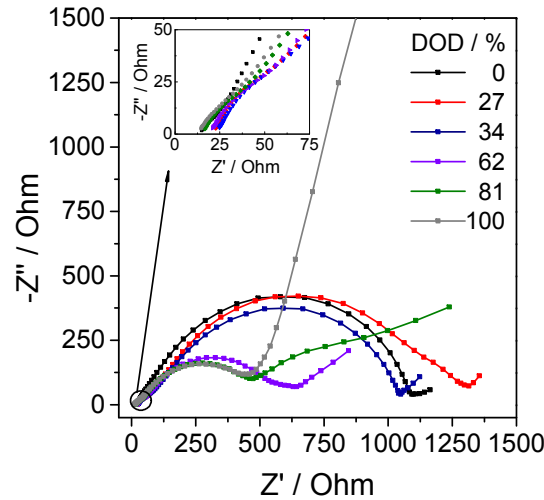
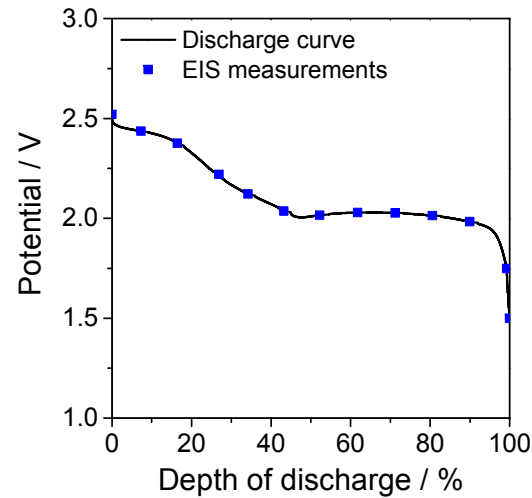


Assignment of processes to the elements of the EC

Model	Chemical and physical cause
R_0	Ohmic resistance
R_1 - CPE_1	Anode charge transfer
R_2 - CPE_2	Cathode process: charge transfer of sulfur intermediates
R_3 - CPE_3	Cathode process: reaction and formation of S_8 and Li_2S
R_4 - CPE_4	Diffusion



EIS during 1st discharging cycle



R_0 : Increase of resistance due to dissolution of Li_2S_x

R_1 : Anodic charge transfer resistance influenced by Li_2S_x

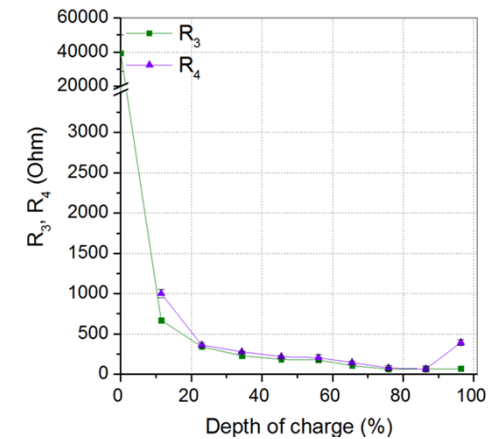
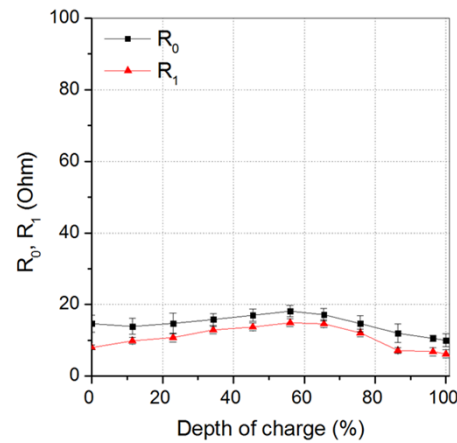
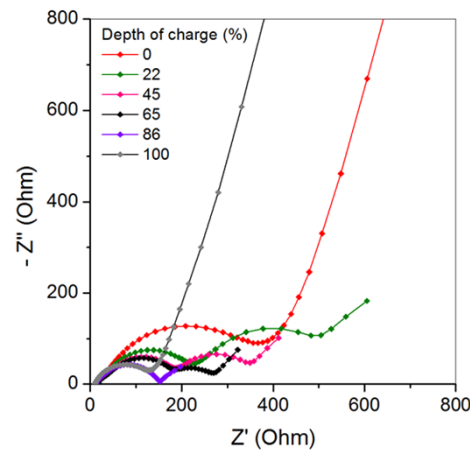
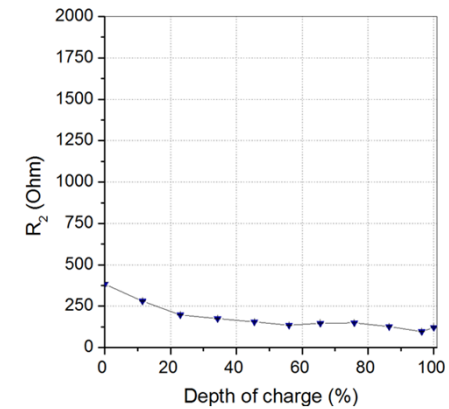
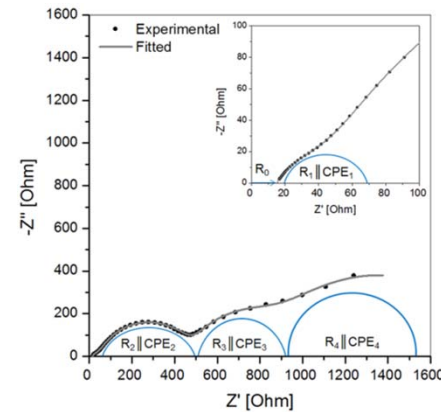
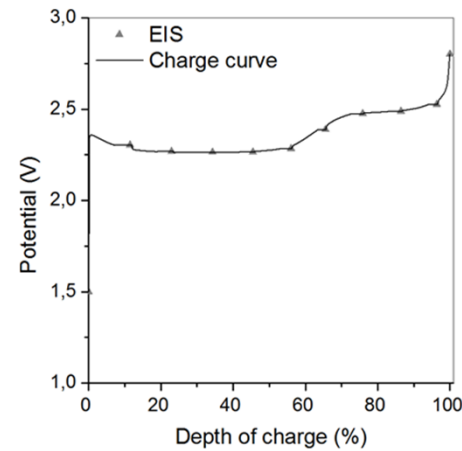
R_2 : Cathodic charge transfer resistance diminishes with order or polysulfide

R_3 : Proportional to formation of isolating products (Li_2S and S_8)

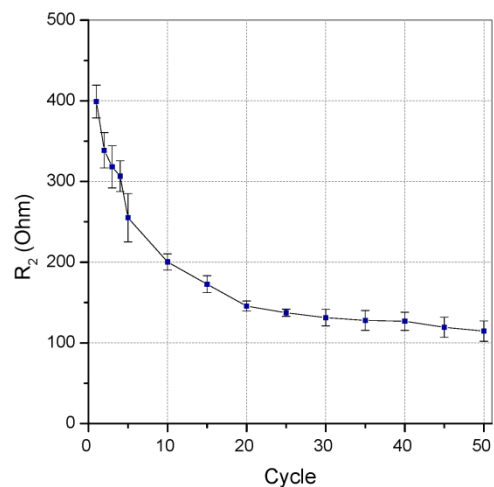
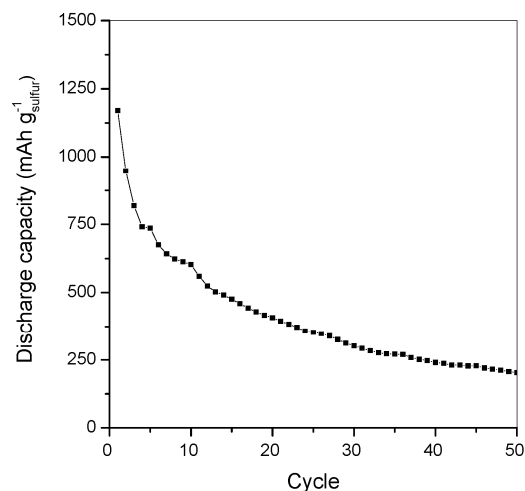
R_4 : Diffusion hindered by formation of Li_2S and S_8



Variation of the equivalent circuit elements during first charging determined by EIS analysis



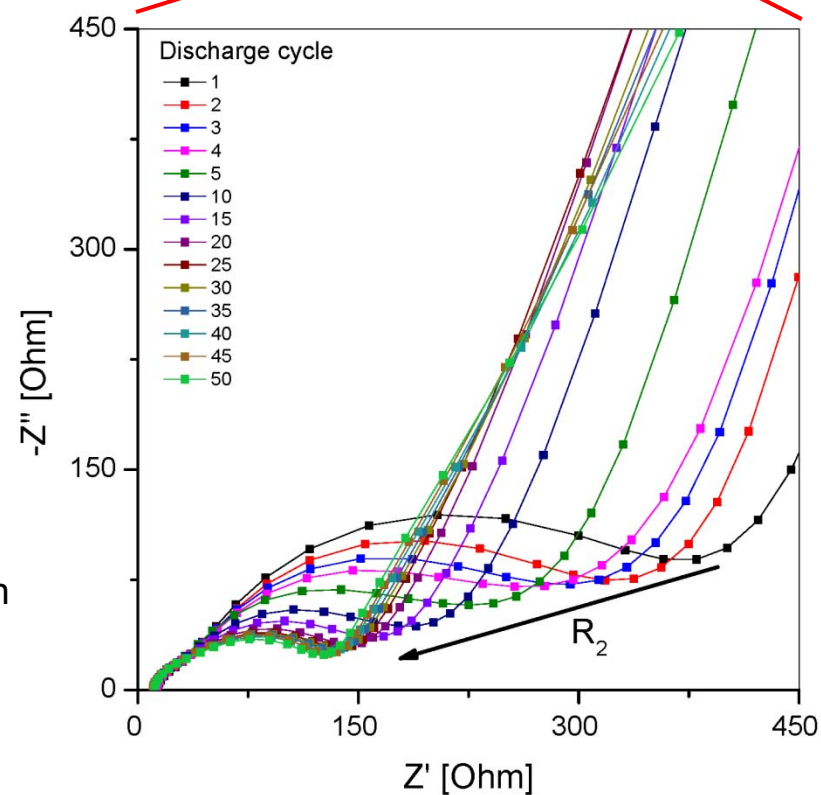
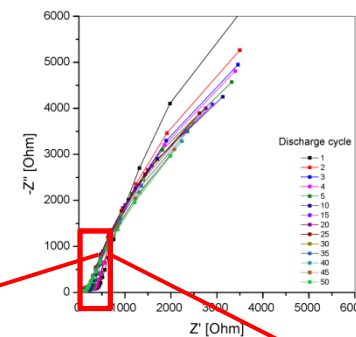
EIS during 50 charging/ discharging cycle



Strong
discharge
capacity fading

Decrease of
cathodic charge
transfer (R_2)

No complete conversion
to Li_2S



New batteries concepts

Further cathode improvements

Components

- Electrolyte/sulfur weight ratio: $\leq 3/1$
- Mass loading higher than 2 mg cm^{-2}
- Sulfur utilization $\geq 70 \%$

Different approaches or combination of them:

- **Additives:** hydrophilic inorganic additives (like Me_xO_y) for adsorption of polysulfides
- **Protective layers:** ion conductive interlayers for retention of active material
- **Binders:** replacement of conventional PVDF by ion /electric conductive additive

Guideline for an optimized electrode and cell design:

- Modeling from a single active particle to full battery cells
- Mechanistic studies of degradation processes on both electrodes



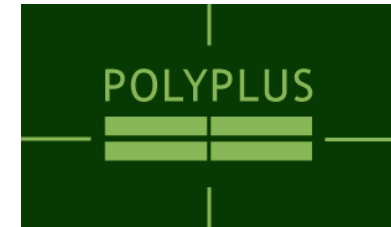
Main companies developing Li/S Batteries in industry



Abingdon, UK



Tucson, USA



Berkeley, USA

Target for commercialization: ca. 500 Wh/kg

Oxis Energy:

- 300 Wh/kg achieved at cell level in 2014
- 400 Wh/kg forecast in 2016

Sion Power:

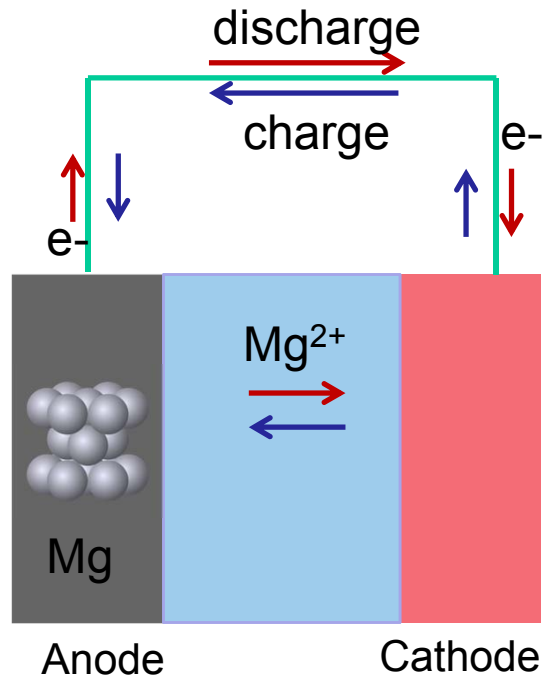
- 250 Wh/kg and over 300 full depth of discharge cycles (now)
- 600 Wh/kg are in the foreseeable future



<http://www.oxisenergy.com/technology/>
<http://www.sionpower.com/>
<http://www.polyplus.com/>



Li-Sulfur vs. Mg-Sulfur Battery

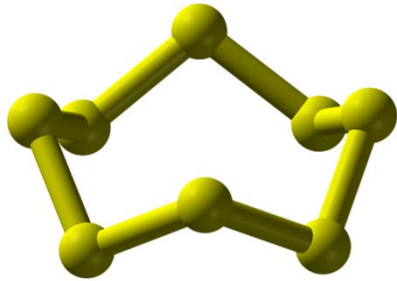


	Li	Mg
Atomic weight	6.9	24.3
Ionic radius	90 pm	86 pm
Ionic charge	+ 1	+ 2
Reduction potential	- 3.04 V	- 2.37 V
Density	0.53 g/cm ³	1.74 g/cm ³
Gravimetric capacity	3861 mAh/g	2205 mAh/g
Volumetric capacity	2061 mAh/cm ³	3832 mAh/cm ³

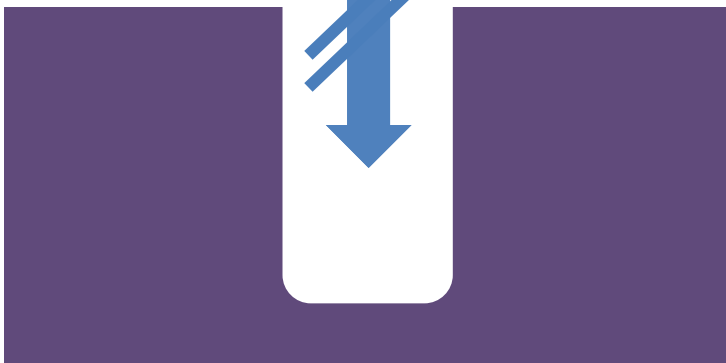
- Good handling and operational safety
- No dendrite formation using Mg metal as anode
- Naturally abundant → low raw material cost (currently Li/25)
- Mg/S offers theoretical 4000 Wh/L while the gravimetric capacity is similar to that of LiC₆
- Sulfur cathode needs non-nucleophilic electrolyte



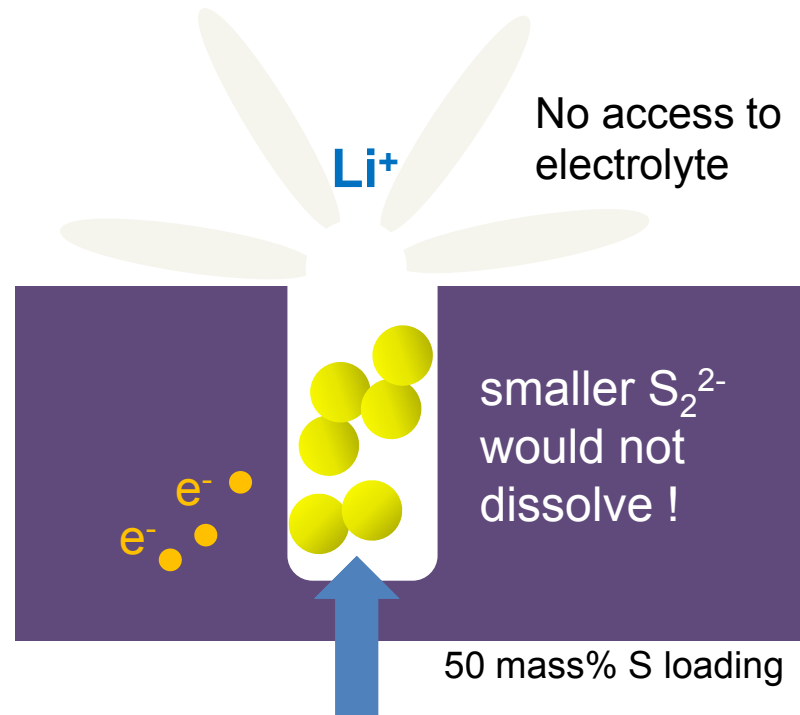
Reduction of polysulfide shuttle



S_8 and soluble S_8^{2-}
do not fit in pore



Ultramicroporous carbon
made from coconut shells
(inexpensive, scalable).
Pore $\varnothing \approx 0.6$ nm



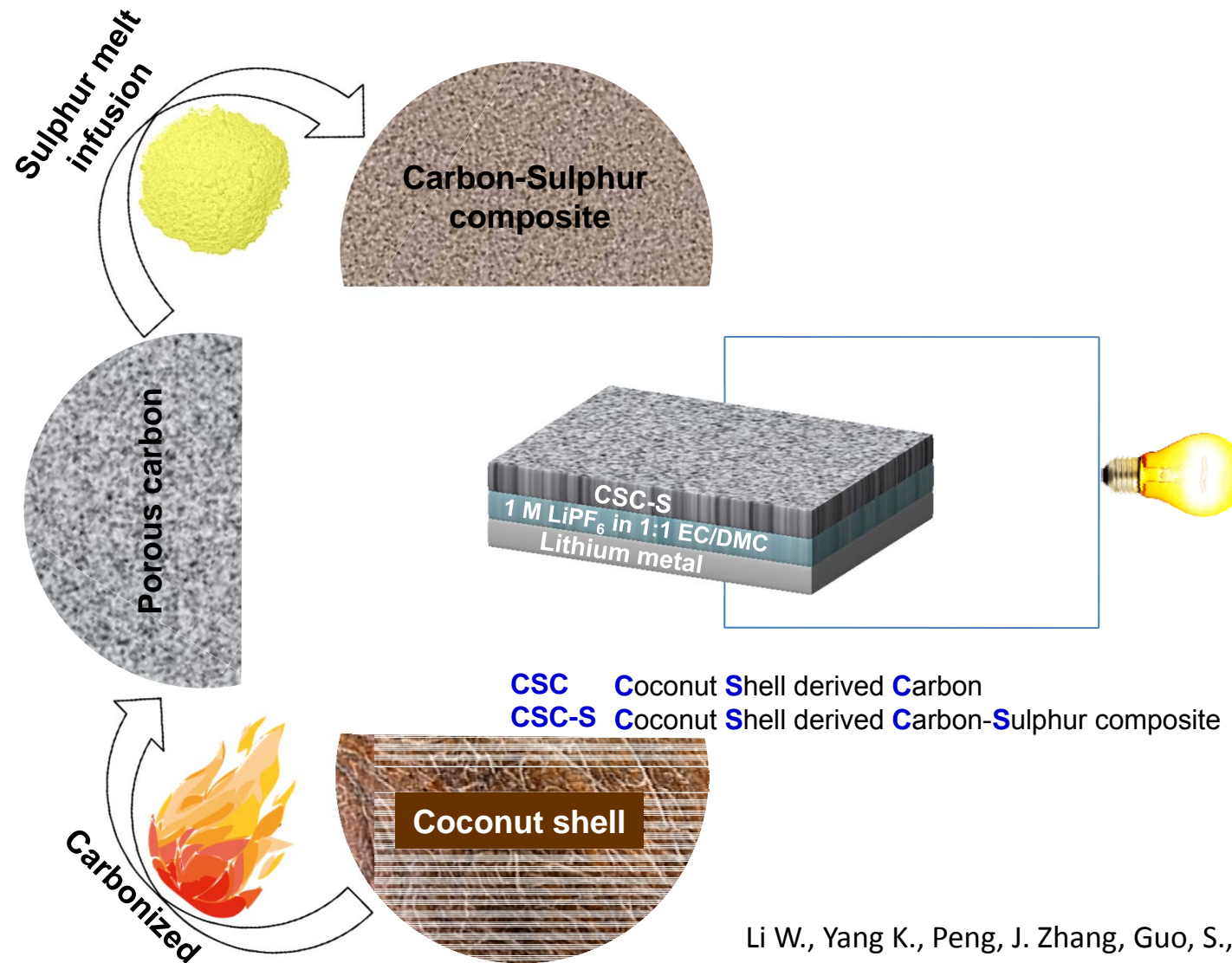
Hypothesis:

direct transition of S to Li_2S_2 and Li_2S

one reaction step \rightarrow one plateau



Production of Carbon-Sulfur Composite



Li W., Yang K., Peng, J. Zhang, Guo, S., Xia, H.
Ind. Crop. Prod. **28**, 190–198 (2008).



Metal-air batteries



Motivation

Why Li-air batteries?

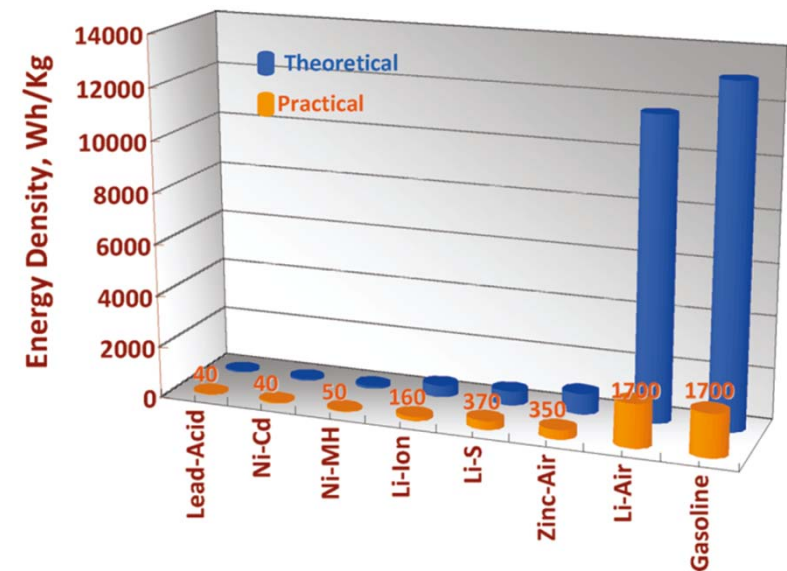
- Highest theoretical specific energy density (11.425 Wh/kg)
Cathodic reactant, O_2 from air, does not have to be stored
- Environmental friendliness
- Higher safety than Li-ion batteries
(only one of the reactants contained in the battery)
- Potentially longer cycle and shelf lives



Motivation

Why Li-air batteries?

- Highest theoretical specific energy density (11.425 Wh/kg).
Cathodic reactant, O_2 from air, does not have to be stored
- Environmental friendliness
- Higher safety than Li-ion batteries
(only one of the reactants contained in the battery)
- Potentially longer cycle and shelf lives



G. Girishkumar et al., J. Phys. Chem. Lett.,
2010, 1, 2193-2203



Li-air battery: Functional scheme

Structure:

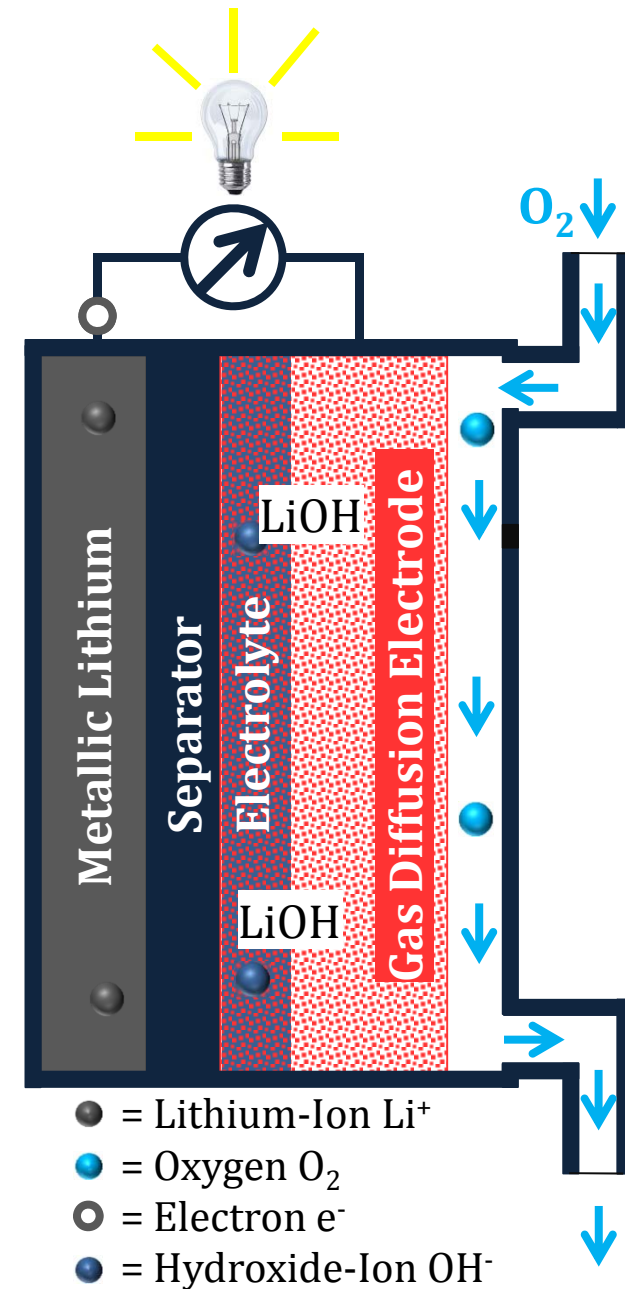
- Anode, Lithium metal (foil)
- Cathode (Gas diffusion electrode = GDE)
- Separator

Reactions and products:

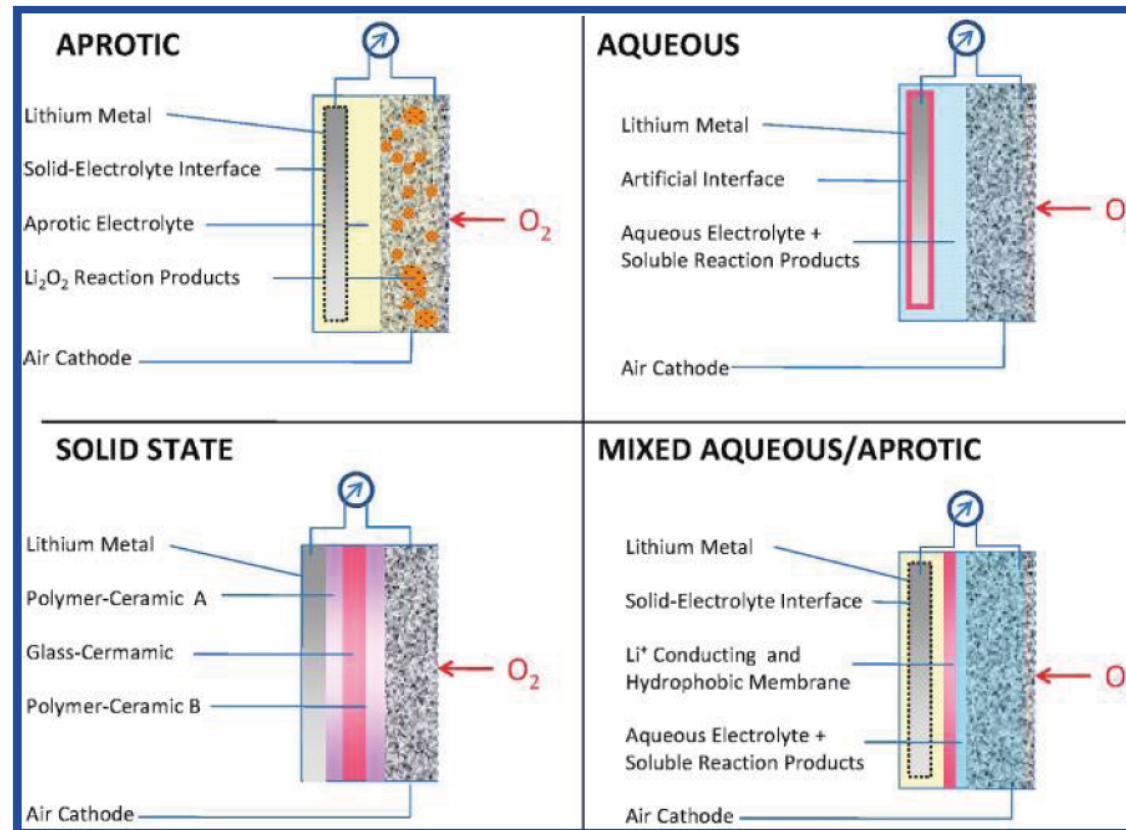
- During discharge: Oxygen Reduction Reaction (ORR)
- During charging: Oxygen Evolution Reaction (OER)
- Reaction product:
 - organic electrolyte: Li_2O , Li_2O_2
 - alkaline electrolyte: LiOH

DLR:

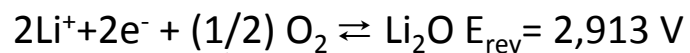
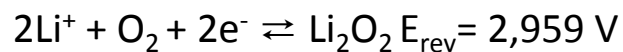
- Bifunctional Cathode (GDE) with alkaline electrolyte (LiOH)
- Global reaction: $4 \text{Li} + \text{O}_2 + 2 \text{H}_2\text{O} \leftrightarrow 4 \text{LiOH}$;
 $E=3.45\text{V}$



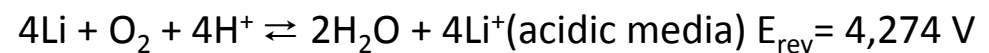
Architectures of Li-air Batteries



Non-aqueous electrolyte:

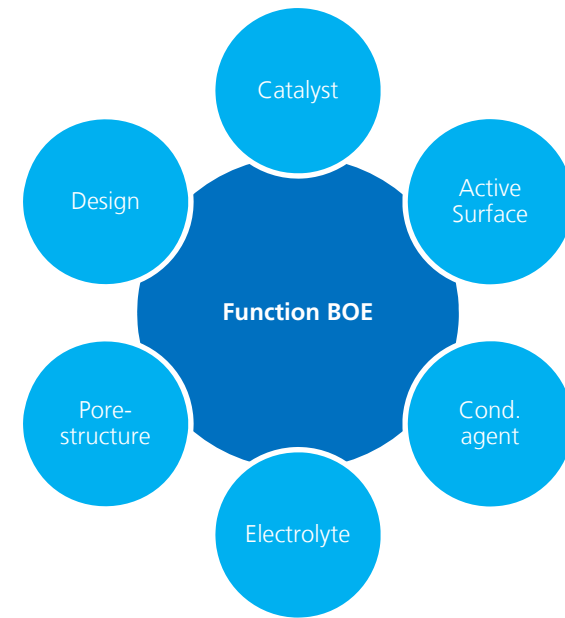
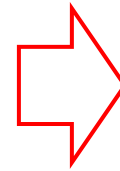
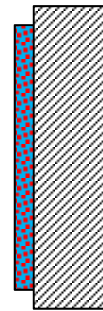


Aqueous electrolyte:

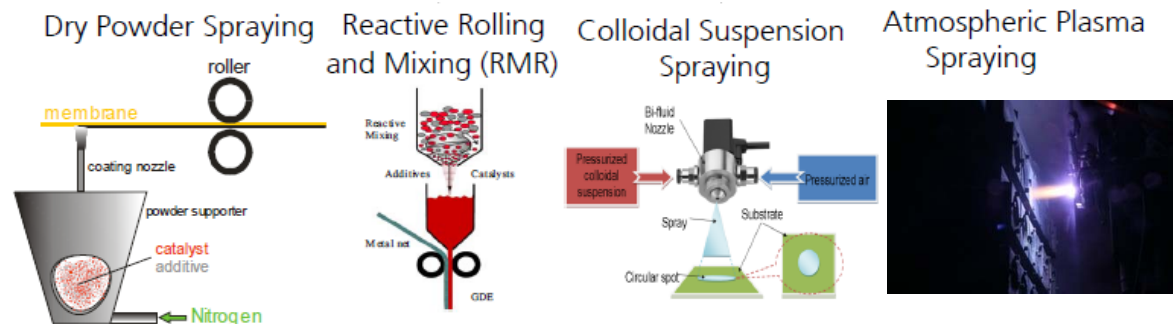


Bi-functional Oxygen-Electrodes: Design

- Bi-functional Oxygen-Electrodes = catalyzes ORR and OER
- Depending on manufacturing process every electrode consists of:
 - Catalyst(s)
 - Conductive agent (C, Graphit...)
 - Binder (PTFE, PVdF...)
 - Substrate (Metal mesh,...)



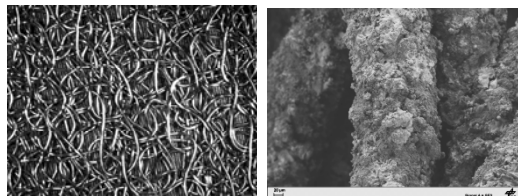
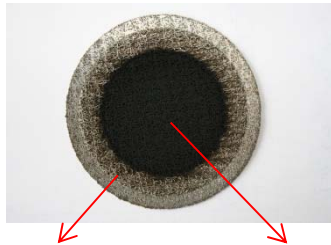
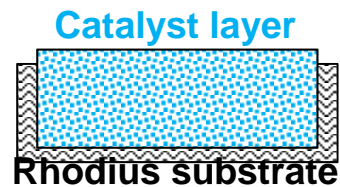
- Different manufacturing processes used at DLR: Dry Powder Spraying, Reactive Rolling and Mixing (RMR), Colloidal Suspension Spraying, and Atmospheric Plasma Spraying



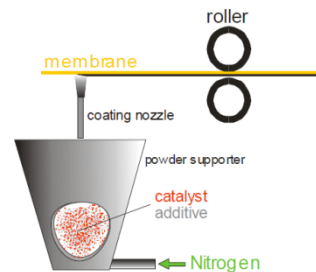
Manufacturing of bifunctional gas diffusion electrodes

Oxide catalysts

($\text{La}_{0.6}\text{Ca}_{0.4}\text{CoO}_{3\dots}$) can be sprayed on for example a Rhodius substrate with APS



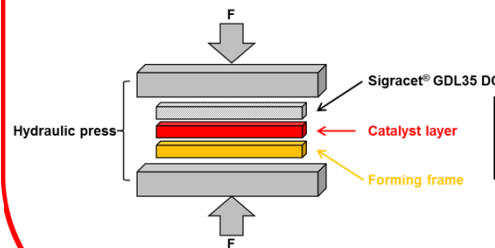
Electrodes with **noble metal** and **other catalysts** can be made with dry power spraying technique



**Catalyst layer =
catalyst+carbon/graphite+binder**
Graphite GDE substrate



or by pressing the catalyst layer on for example a Sigracet® GDL 35 DC with a hydraulic press



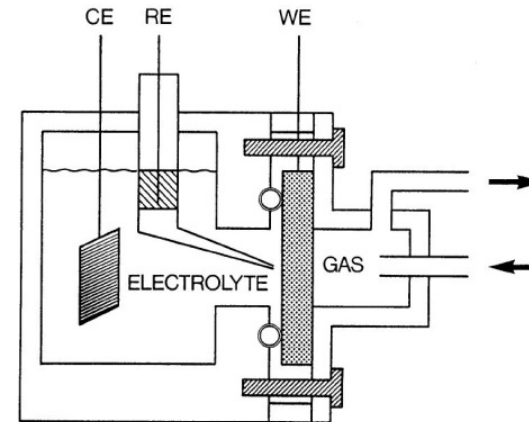
**Catalyst layer =
catalyst+carbon/graphite+binder**
Sigracet® GDL35 DC



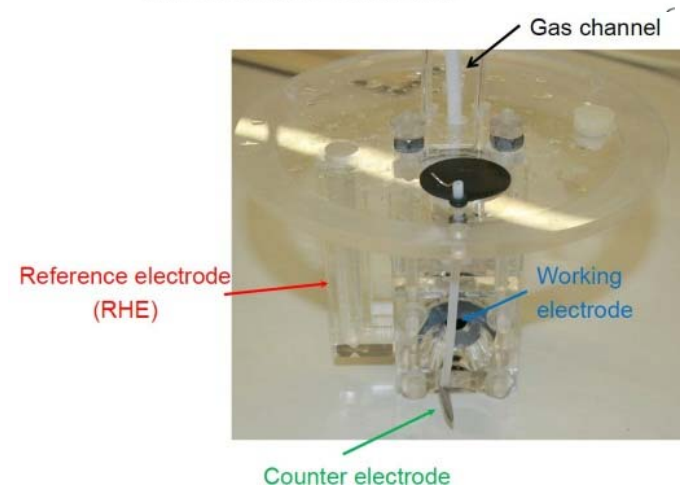
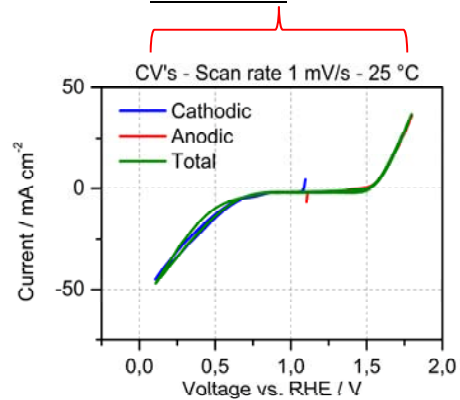
Screening of bifunctional catalysts

Experimental

- Thin catalyst layers reduce the influence of the electrode structure
- Cyclic Voltammetry was carried out at a half cell with 1M LiOH (aq.) and 25° C and 50° C
- Gas O_2 , platinum counter electrode (CE), reversible hydrogen reference electrode (RE)



Potential range 0.1V - 1.8V
vs. RHE



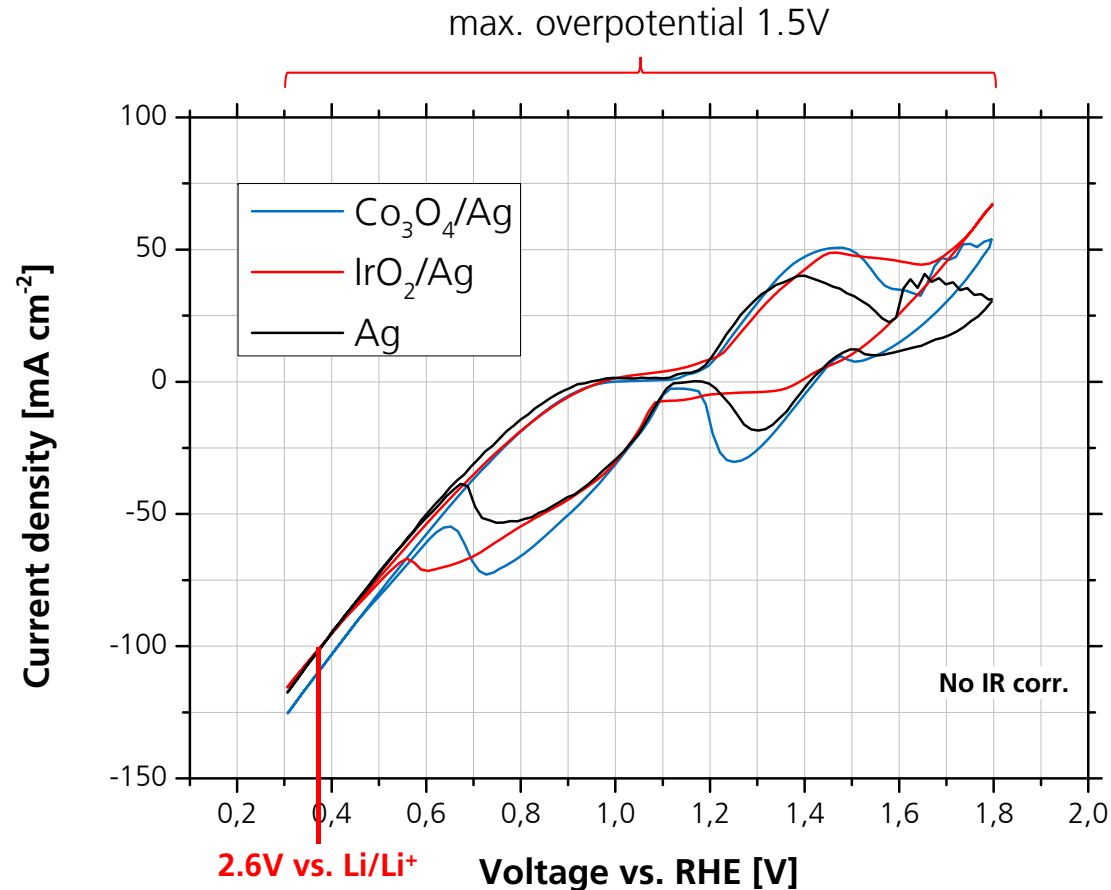
Bi-functional Oxygen-Electrodes: IrO₂/- and Co₃O₄/Ag-electrodes

- CV's electrodes 20 wt. % catalyst (IrO₂, Co₃O₄)
- Improved cycling performance due to use of IrO₂ and Co₃O₄ compared to pure Ag

Current density @ 2.6V
vs. Li/Li⁺ [mA cm⁻²]

IrO₂/Ag 99,7

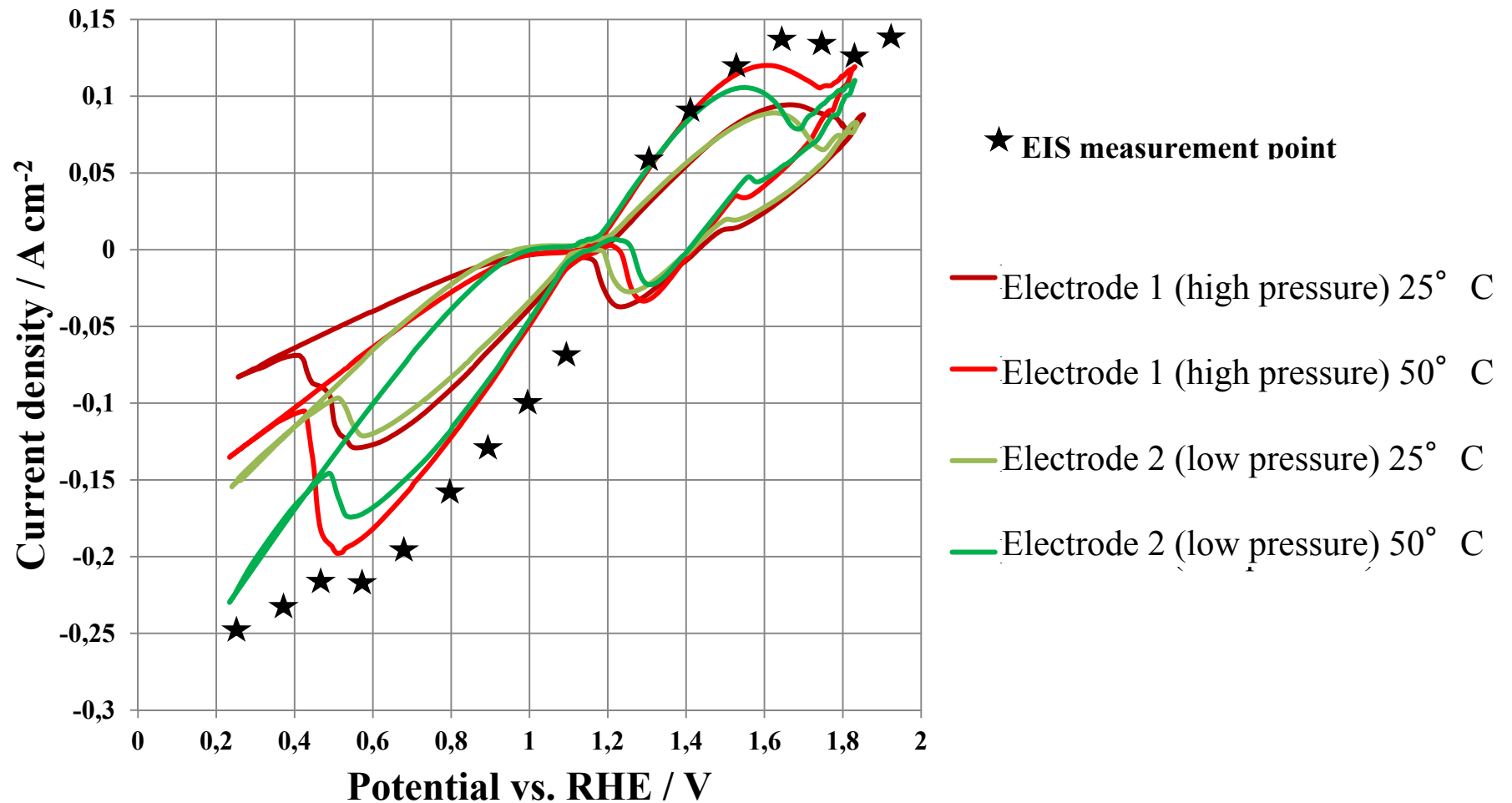
Co₃O₄/Ag 107



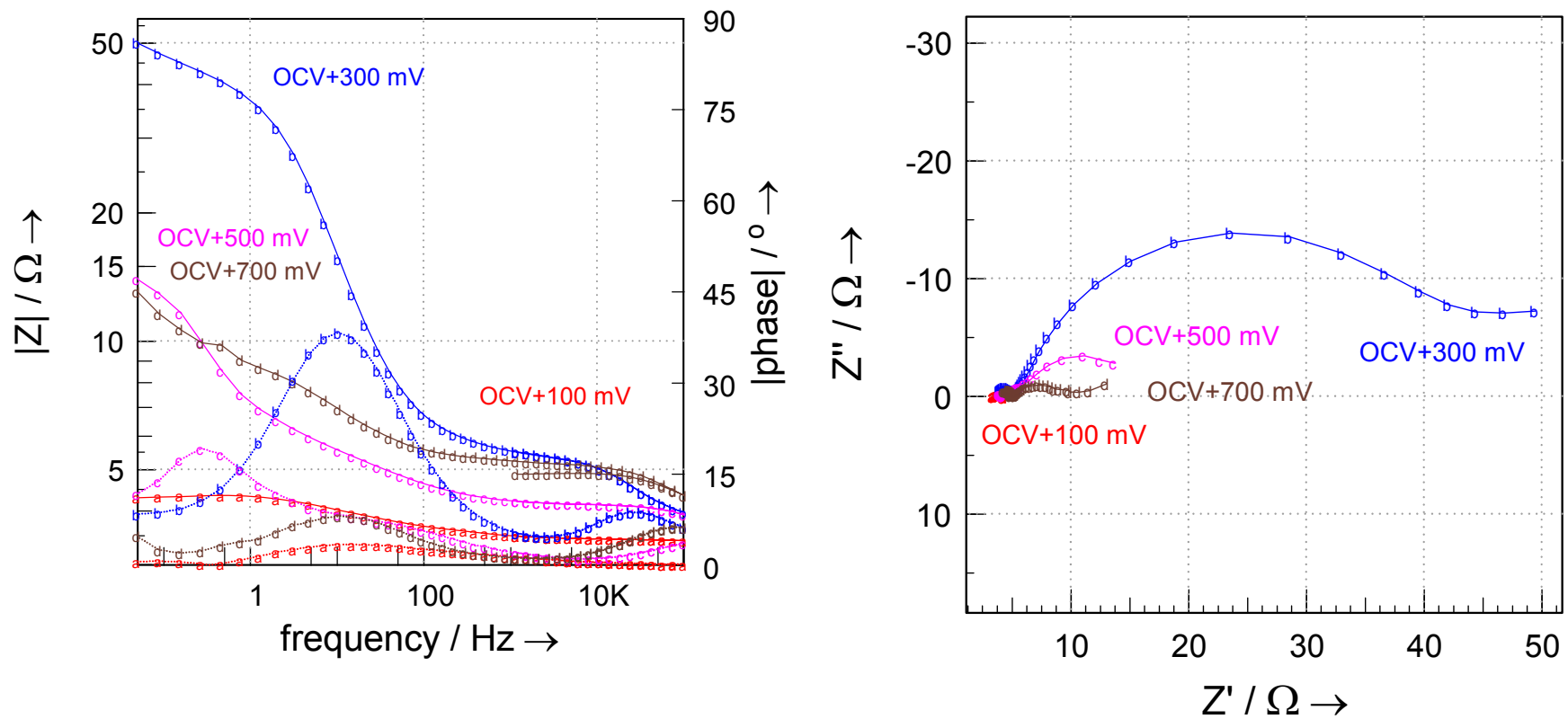
N. Wagner , D. Wittmaier, German Patent Application, 2014



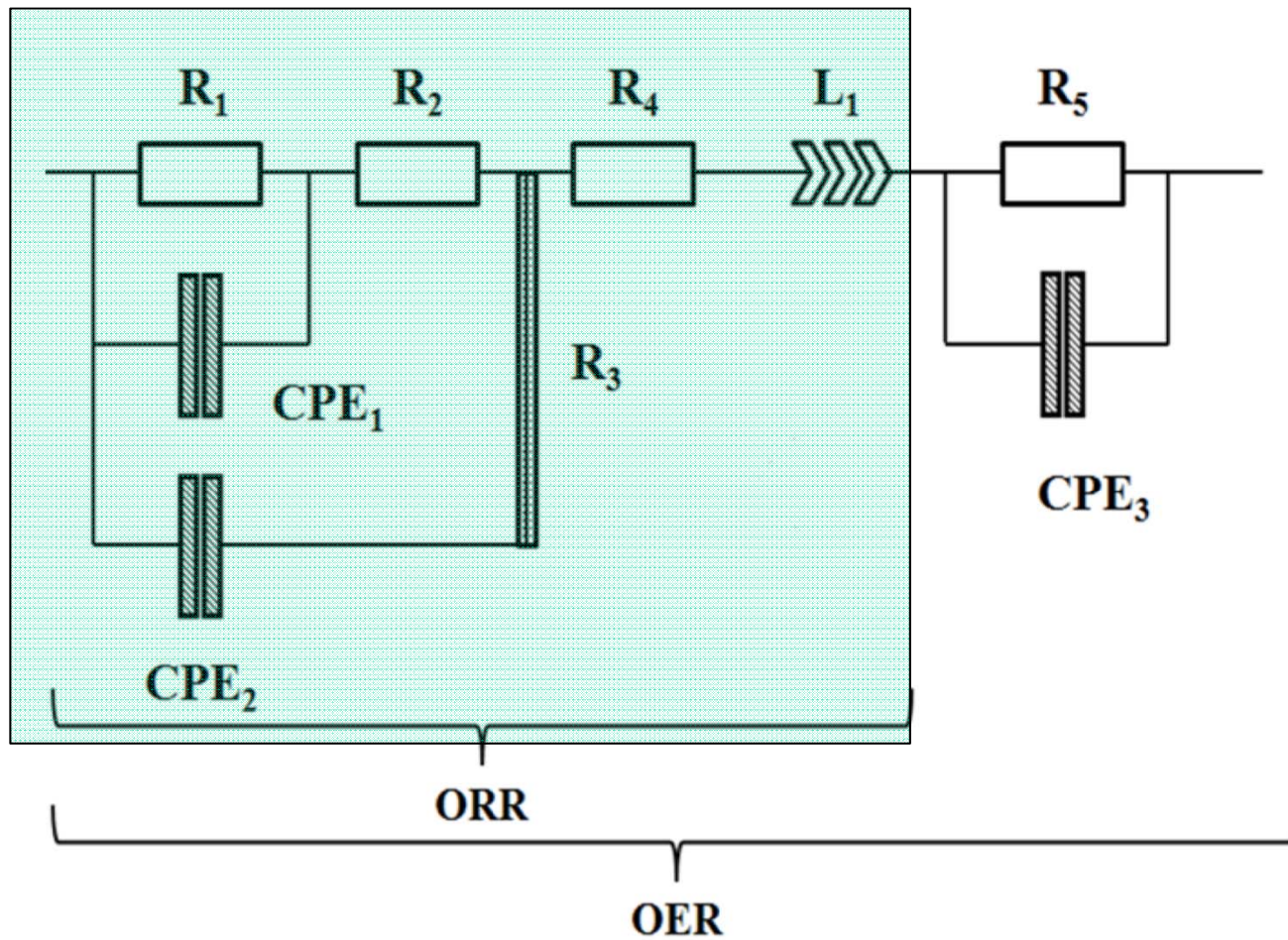
Overview EIS measurement points and CV with 1 mV/s at RT, 1 N LiOH , Ag-GDE



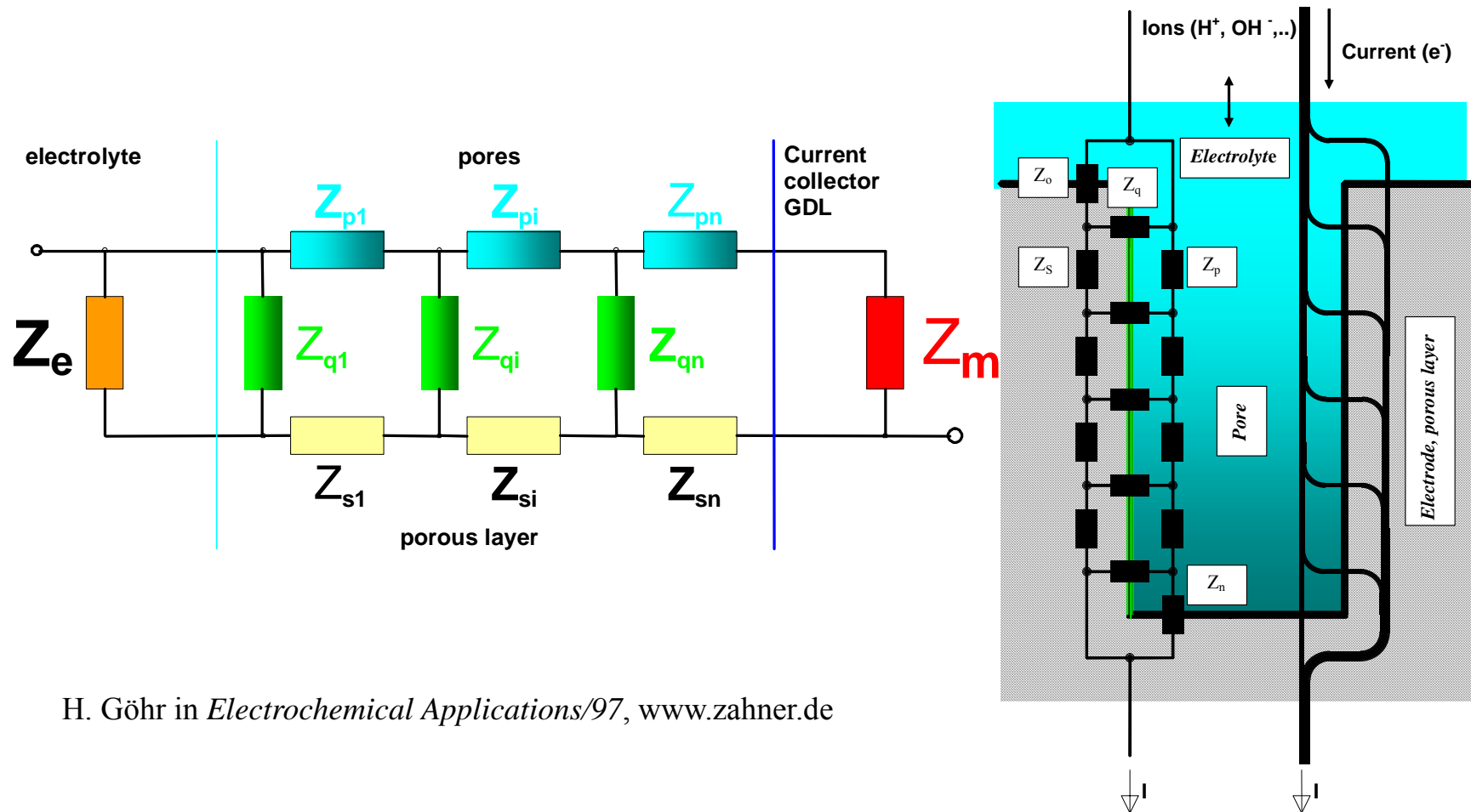
Impedance measurements during Oxygen evolution on Ag-GDE (high pressure), 1 N LiOH, 25° C



Equivalent circuit used for evaluation of EIS during OCR and OER at different electrodes for Lithium-Air batteries



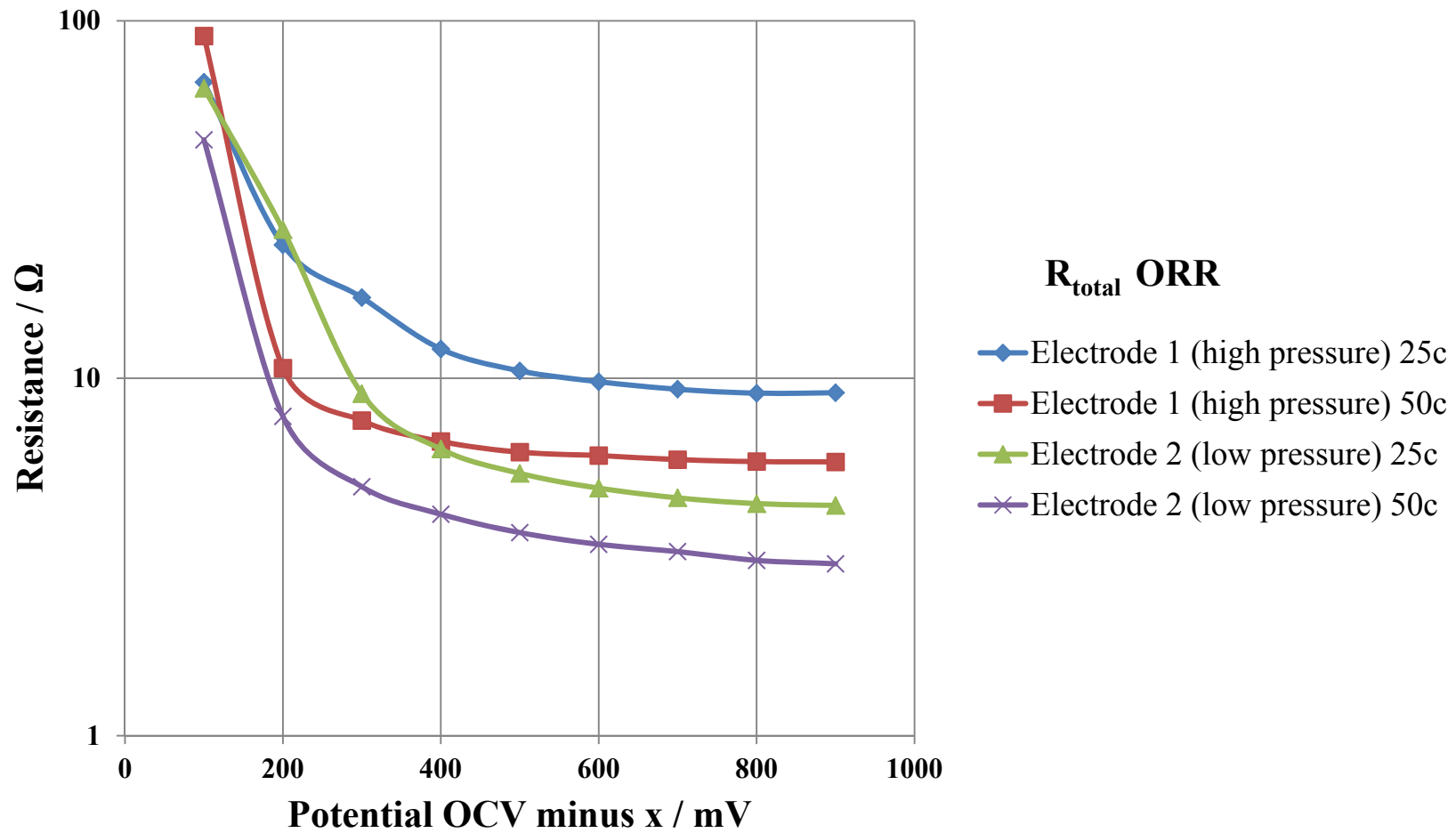
Cylindrical homogeneous porous electrode model (H. Göhr)



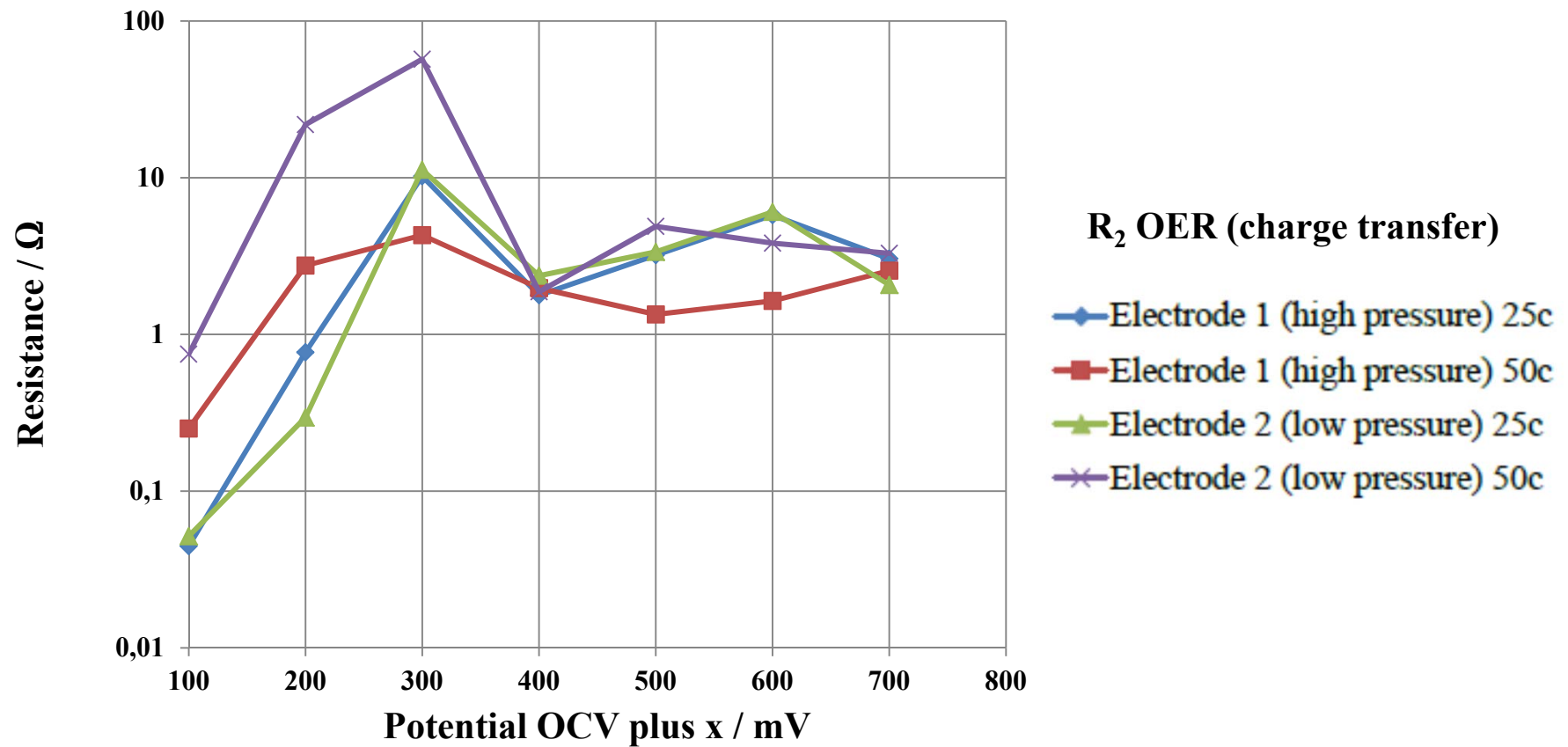
H. Göhr in *Electrochemical Applications/97*, www.zahner.de



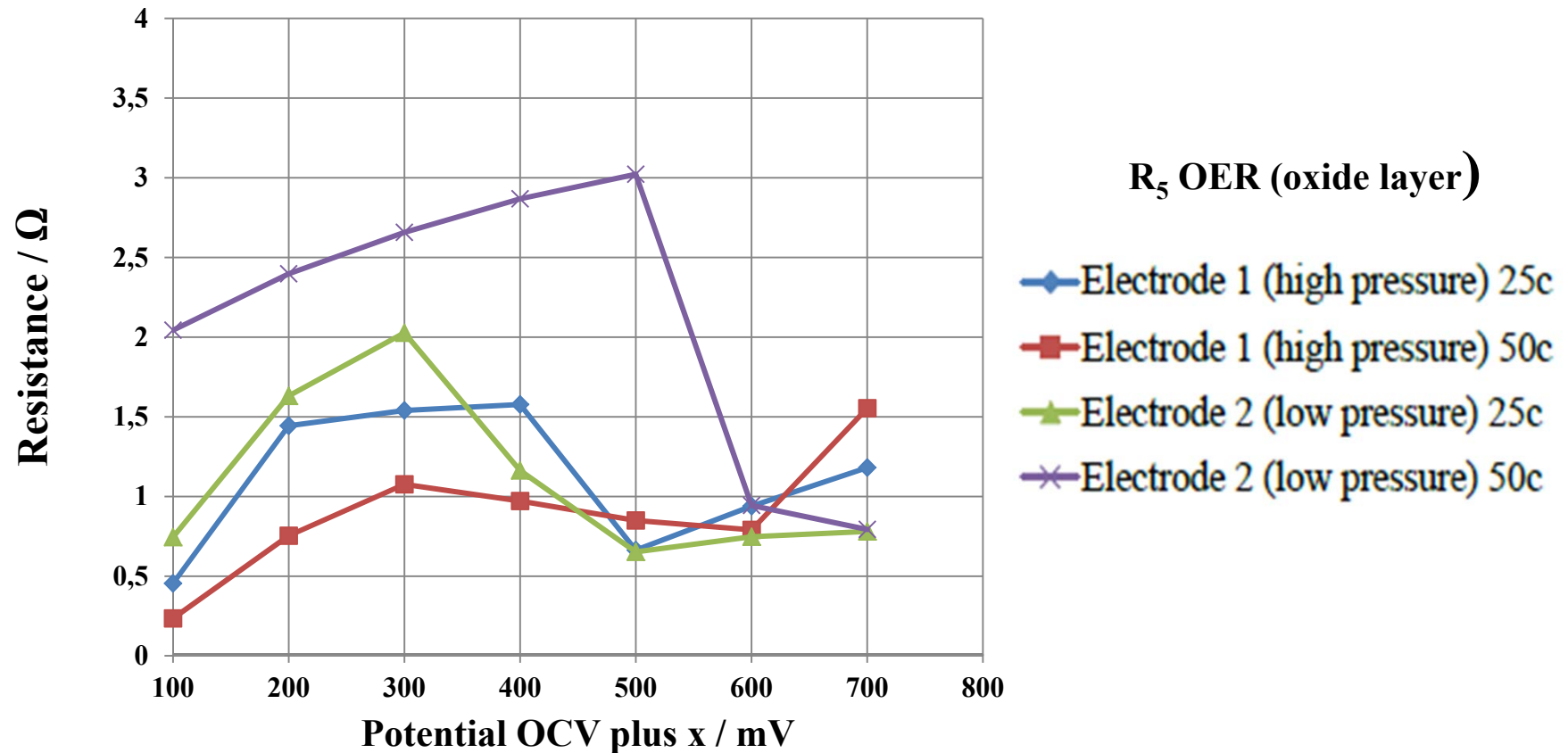
Potential dependency of total resistance during ORR at different electrodes, 1 N LiOH



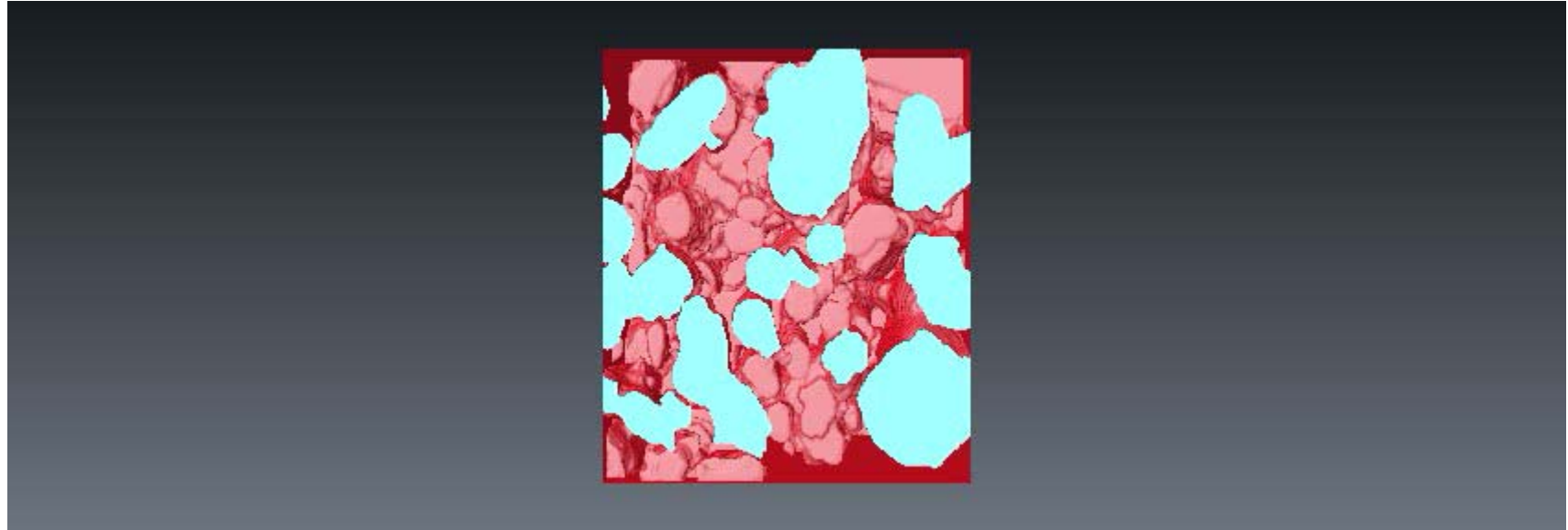
Potential dependency of charge transfer resistance during OER



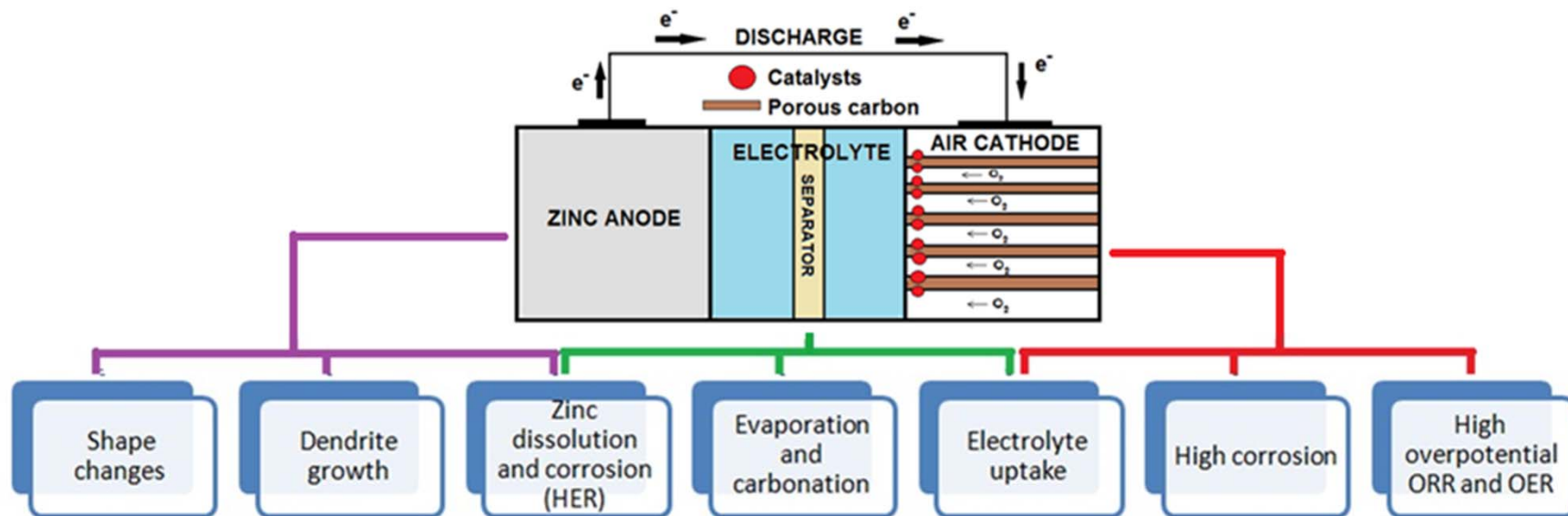
Potential dependency of charge transfer resistance in oxide layer potential region (OER)



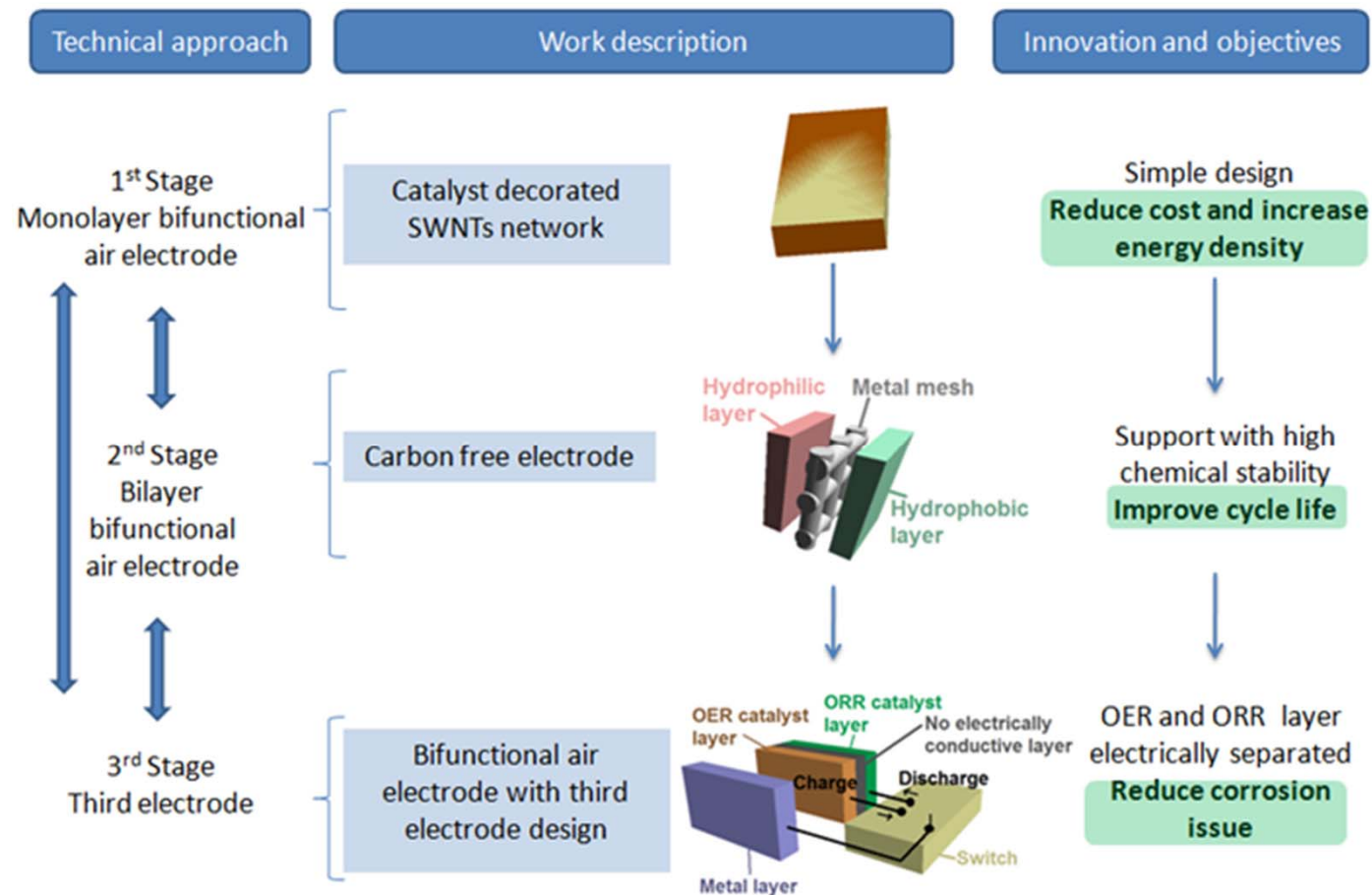
FIB-TEM picture of a Silver gas diffusion electrode



Main Limitations of the Zinc-Air Battery



“ZAS” innovation on the bifunctional air electrode



**German Aerospace
Center (DLR)**

Institute of
Engineering
Thermodynamics



Battery group

Thank you for your attention!
Vielen Dank für Ihre Aufmerksamkeit!
Gracias por su atención!
Multumesc pentru atenție!

